Biochemical analysis and genetic engineering of oleaginous fungi for the production of eicosapentaenoic acid and free fatty acid derivatives

Brian King Himm Mo

2021

CONTENTS

ABBREVIATIONS …4

GENERAL INTRODUCTION …6

CHAPTER 1

Characterization of ω3 fatty acid desaturases from oomycetes and their application toward eicosapentaenoic acid production in *Mortierella alpina* …7

CHAPTER 2

Establishment of a platform organism *Basidiobolus meristosporus* for free fatty acid derivative production …43

SECTION 1

Free fatty acid production by the oleaginous fungus *Basidiobolus meristosporus* …43

SECTION 2

Development of a host-vector system for free fatty acid derivative production by *Basidiobolus meristosporus* …57

CONCLUSIONS …83

ACKNOWLEDGEMENTS …85

PUBLICATIONS …86

ABBREVIATIONS

12:0	Lauric acid
13-OH LA	13-Hydroxy-*cis*-9-octadecenoic acid
14:0	Myristic acid
14:1	Myristoleic acid
16:0	Palmitic acid
16:1	Palmitoleic acid
18:0	Stearic acid
18:1	Oleic acid
18:2	Linoleic acid
18:3	γ-linolenic acid
ALA	α-linolenic acid
ARA	Arachidonic acid
ATMT	*Agrobacterium tumefaciens*-mediated transformation
bp	Base pair(s)
cDNA	Complementary DNA
DAG	Diacylglycerol
DCW	Dry cell weight
DGLA	Dihomo-γ-linolenic acid
DHA	Docosahexaenoic acid
DNA	Deoxyribonucleic acid
EPA	Eicosapentaenoic acid
ETA	Eicosatetraenoic acid
FAME	Fatty acid methyl ester
FFA	Free fatty acid
GC	Gas chromatography
GCMS	Gas chromatography-mass spectrometry
GLA	γ-linolenic acid
GUS	β-glucuronidase gene
GY	Glucose yeast extract

kb	Kilobase(s)
LA	Linoleic acid
MUG	4-methylumbelliferyl-β-D-glucuronide
OA	Oleic acid
PCR	Polymerase chain reaction
PDA	Potato dextrose agar
PL	Polar lipid
PNP	*p*-nitrophenol
PUFAs	Polyunsaturated fatty acids
RNA	Ribonucleic acid
S	Sterol
SDA	Stearidonic acid
SE	Sterol ester
TAG	Triacylglycerol
TFA	Total fatty acid
TLC	Thin layer chromatography
WT	Wild type
YPD	Yeast extract peptone dextrose

GENERAL INTRODUCTION

Modern society relies on various unsustainable sources for the production of chemicals and materials. For example, the main source of dietary functional lipids are rapidly depleting marine fisheries, and the main source of oleochemicals and materials are fossil resources. Due to increasing concerns on climate change, environmental problems, and the depletion of fossil resources, the search for alternative sources has been a focus of current research.

Industrial biotechnology has explored the utilization of microorganisms as cell factories for the production of functional lipids, oleochemicals and fuels from renewable lignocellulosic biomass as raw materials. The model organisms *Escherichia coli* and *Saccharomyces cerevisiae* have been most heavily employed for bioproduction due to a thorough understanding of their metabolisms and the presence of a wide range of metabolic engineering tools, but other platform strains may offer improvements in areas such as the utilization of cost-effective substrates, tolerance to harsh fermentation conditions, and innate productivity of the target compound.

Compared to the traditional workhorses *E. coli* and *S. cerevisiae*, oleaginous fungi (Fungi that can accumulate >20% of biomass as lipids) have greater innate ability to accumulate significant amounts of oil, and are potentially cost-effective sources for the production of functional lipids, oleochemicals and fuels.

This study thus focuses on the development of oleaginous fungi for the production of the functional lipid eicosapentaenoic acid (Chapter 1) and free fatty acid derived-oleochemicals and fuels (Chapter 2). Chapter 1 focuses on the screening of genetic resources for eicosapentaenoic acid production and their application in the oleaginous fungus *Mortierella alpina.* Chapter 2.1 and 2.2 focus on the development of an oleaginous fungus *Basidiobolus meristosporus* for use as a new potential production host for free fatty acid derived oleochemicals and materials.

CHAPTER 1

Characterization of ω3 fatty acid desaturases from oomycetes and their application toward eicosapentaenoic acid production in *Mortierella alpina*

ABSTRACT

ω3 polyunsaturated fatty acids are currently obtained mainly from fisheries; thus, sustainable alternative sources such as oleaginous microorganisms are required. Here, the isolation, characterization, and application of three novel ω3 desaturases with ω3 polyunsaturated fatty acid-producing activity at ordinary temperatures (28 °C) is described. First, *Pythium sulcatum* and *Plectospira myriandra* were selected after screening for oomycetes with high eicosapentaenoic acid/arachidonic acid ratios and the genes *psulω3* and *pmd17,* which encode ω3 desaturases, were isolated. Subsequent characterization showed that PSULω3 exhibited ω3 desaturase activity on both C18 and C20 ω6 polyunsaturated fatty acids while PMD17 exhibited ω3 desaturase activity exclusively on C20 ω6 polyunsaturated fatty acids. Expression of *psulω3* and *pmd17* in the arachidonic acid-producer *Mortierella alpina* resulted in transformants that produced eicosapentaenoic acid/total fatty acid values of 38% and 40%, respectively, at ordinary temperatures. These ω3 desaturases should facilitate the construction of sustainable ω3 polyunsaturated fatty acid sources.

INTRODUCTION

ω3 Polyunsaturated fatty acids (ω3 PUFAs) are essential for human health. Eicosapentaenoic acid (EPA, 20:5ω3) and docosahexaenoic acid (DHA, 22:6ω3) in particular are involved in the inflammatory response, reproduction, blood pressure regulation, cholesterol metabolism, and infant retinal and brain development (1, 2). EPA and DHA are also required parts of human diets, since humans lack the capacity to produce them *de novo* (3). Currently, the main sources of EPA and DHA for humans are fish and seafood (4, 5). However, due to the rising demand for fish and the declining growth of capture and aquaculture fisheries (6), it is expected that these seafood sources will become unsustainable sources of EPA and DHA in the future (7).

Due to these concerns, recent research has been directed toward the development of alternative land-based EPA and DHA sources for aquaculture fish feed and human consumption. Several groups have reported DHA bioproduction at industrial levels, most notably in transgenic canola (8) as well as the microalgae *Crypthecondinium, Schizochytrium*, and *Ulkenia* (9, 10). In contrast, industrially relevant EPA bioproduction has been limited. Various types of endogenous and non-endogenous EPA producers have been reported, including bacteria (11), algae (12, 13), protists (14, 15), fungi (16, 17), oomycetes (18–21), and plants (22–24), all of which do not produce EPA at levels required for commercialization. Until now, a *Yarrowia lipolytica* strain engineered by Xue *et al.* (17) that produced EPA at levels representing up to 56.6% of total fatty acid (TFA) content remains the sole example of a potential commercial EPA source. Identification of other industrial EPA source replacements has thus been a focus of current research.

Around three decades ago, our group reported the discovery of *Mortierella alpina* 1S-4, an oleaginous fungus that accumulates arachidonic acid (ARA, 20:4ω6) under ordinary conditions (28 °C) and EPA under low-temperature cultivation conditions (16, 25, 26) (**Figure 1.1**). In order to more thoroughly understand its PUFA metabolism and heterologously overproduce PUFAs, our group developed methods for selection (27, 28), transformation (29, 30), regulatory element manipulation (31, 32), and gene targeting (33). This enabled the overexpression of the ω3 desaturase gene of *M. alpina* 1S-4, which catalyzes the desaturation of ω6 fatty acids to ω3 fatty acids, resulting in a transformant with 40% EPA/TFA (30). However, EPA accumulation required cultivation at 12 °C, the optimal condition for ω3

desaturase gene expression. Since low-temperature cultivation negatively impacts fatty acid productivity and necessitates cooling during fermentation, circumventing low-temperature cultivation has been another recent research focus (34–36). The expression of ω3 desaturases with activity at ordinary temperatures is expected to increase EPA production since *M. alpina* accumulates approximately 70% of TFAs as C20 ω6 PUFAs (25) under ordinary temperatures.

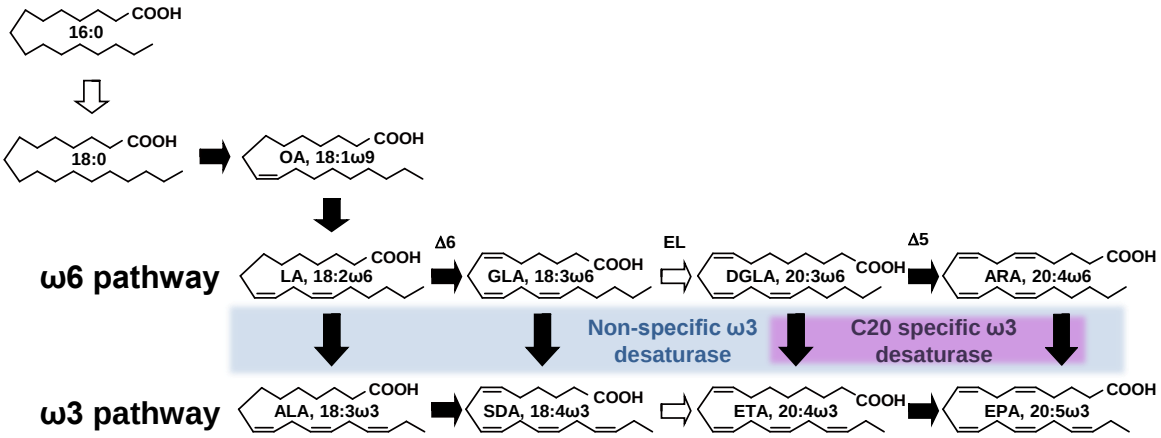

Figure 1.1. The elongase and desaturase PUFA biosynthetic pathway of *M. alpina* with expressed oomycete-derived desaturases highlighted. Δ6, Δ6 desaturase; Δ5, Δ5 desaturase; EL, elongase; OA, oleic acid; LA, linoleic acid; ALA, α-linolenic acid; GLA, γ-linolenic acid; SDA, stearidonic acid; DGLA, dihomo-γ-linolenic acid; ETA, ω3 eicosatetraenoic acid; ARA, arachidonic acid; EPA, ω3 eicosapentaenoic acid. Black arrows, desaturases; white arrows, elongases.

As ω3 desaturases exhibit varying levels of substrate specificity toward C18 and C20 fatty acids (37–43), careful selection of an ω3 desaturase suitable for the overexpressed pathway is necessary. For instance, in *M. alpina* EPA could be produced using two strategies; the insertion of ω3 desaturases catalyzing the desaturation of C18 and C20 fatty acids (henceforth referred to as "non-specific ω3 desaturases") would increase the overall flux of ω6 to ω3 fatty acids toward EPA. Alternatively, expressing an ω3 desaturase with exclusive activity on C20 fatty acids (henceforth referred to as "C20-specific ω3 desaturases") would convert the endogenously accumulated C20 ω6 fatty acid pool toward EPA with minimal accumulation of C18 ω3 fatty acid byproducts such as α-linolenic acid (ALA, 18:3ω3) and stearidonic acid (SDA, 18:4ω3). Regardless of the strategy employed, the ω3 desaturase

activity needs to be high. Up to now, several non-specific ω3 desaturases (37–39, 41–43) and one C20-specific ω3 desaturase (40) have been identified, but EPA production utilizing these enzymes did not reach levels needed for commercialization. Reports utilizing currently identified ω3 desaturases achieved EPA/TFA values of 31.5% with *Phytophthora parasitica* non-specific ω3 desaturase (34), 26.4% with *Saprolegnia diclina* C20-specific ω3 desaturase (35), and 20% with *P. aphanidermatum* non-specific ω3 desaturase (36). Moreover, no previous studies have examined screening methods for isolating potential microorganisms expressing efficient ω3 desaturases.

The aim of this study was to identify efficient non-specific and C20-specific ω3 desaturases suitable for EPA production based on screening oomycetes using the EPA/ARA ratio. Research focused on the oomycete orders Peronosporales and Saprolegniales, which contain genera known to harbor ω3 desaturases with efficient desaturase activity or high specificity for C20 fatty acids (*Saprolegnia*, *Phytophthora*, and *Pythium*). Three ω3 desaturases from two selected species were cloned for functional analysis in *Saccharomyces cerevisiae* and then expressed in *M. alpina* to evaluate their capability for EPA production.

RESULTS

Screening and cloning of putative ω3 desaturase genes from *Pythium sulcatum* and *Plectospira myriandra*

35 strains belonging to the orders Peronosporales and Saprolegniales (**Table 1.1**) were grown in GY medium for 7 days, and the fungal tissue of 18 strains that showed sufficient growth were harvested. Their intracellular fatty acids contained varying levels of several ω3 and ω6 fatty acids (**Table 1.2**).

Table 1.1. Peronosporales and Saprolegniales strains obtained from NBRC

NBRC no.	Species	NBRC no.	Species
9173	*Phytophthora infestans*	33126	*Pythium porphyrae*
30346	*Pythium irregulare*	33180	*Phytophthora cinnamomi*
30817	*Pythium zingiberis*	100113	*Pythium myriotylum*
30819	*Pythium insidiosum*	100117	*Pythium sulcatum*
31624	*Phytophthora megasperma*	100120	*Pythium torulosum*
31924	*Pythium vanterpoolii*	100125	*Pythium ultimum*
31927	*Pythium volutum*	101781	*Pythium scleroteichum*
31933	*Pythium periplocum*	102125	*Pythiopsis cymosa*
32166	*Pythium torulosum*	102130	*Thraustotheca clavata*
32219	*Pythium aristosporum*	103118	*Pythium catenulatum*
32326	*Phytophthora cryptogea*	104967	*Pythium grandisporangium*
32560	*Pythium pyrilobum*	105919	*Phytophthora sojae*
31935	*Aphanomyces iridis*	102431	*Scoliolegnia cf. asterophora*
32548	*Plectospira myriandra*	104173	*Brevilegnia variabilis*
32606	*Salisapilia tartarea*	104176	*Saprolegnia subterranea*
32618	*Halophytophthora epistomium*	104178	*Dictyuchus sterilis*
32710	*Saprolegnia diclina*	104969	*Halioticida noduliformans*
33107	*Pythium aphanidermatum*		

Table 1.2. Lipid profiles of strains showing sufficient growth in GY medium

NBRC no.	Strain	Proportion of total fatty acids (%)											
		16:0	18:0	OA	LA	GLA	DGLA	ARA	ALA	SDA	ETA	EPA	Other fatty acids
30346	*Pythium irregulare*	19.92	2.59	10.92	21.93	0.89	0.83	9.82	trace	0.11	0.29	11.62	21.08
32219	*Pythium aristosporum*	23.55	3.19	18.64	4.23	1.57	2.81	6.39	0.11	0.60	1.60	6.95	30.37
33107	*Pythium aphanidermatum*	23.62	0.77	15.37	9.43	0.77	1.98	8.01	0.20	0.30	1.15	10.51	27.88
100117	*Pythium sulcatum*	23.01	1.52	19.97	9.67	1.29	0.93	1.54	0.39	1.67	1.73	7.30	30.99
100120	*Pythium torulosum*	18.99	2.63	10.29	17.77	2.60	0.87	8.11	0.48	1.45	0.71	14.05	22.04
100125	*Pythium ultimum*	18.12	1.39	11.04	21.27	1.24	1.11	11.42	trace	0.19	trace	11.72	22.50
103118	*Pythium catenulatum*	23.61	1.08	12.86	13.97	1.10	0.63	7.86	0.27	0.35	0.35	10.14	27.78
32326	*Phytophthora cryptogea*	24.73	0.69	6.97	16.65	1.69	1.76	5.84	trace	0.68	2.53	10.15	28.31
31624	*Phytophthora megasperma*	15.68	2.64	4.10	19.00	1.12	1.19	6.52	trace	trace	2.34	7.28	40.15
33180	*Phytophthora cinnamomi*	28.02	1.51	6.33	16.56	1.23	1.02	11.44	trace	0.05	3.23	3.63	26.98
31935	*Aphanomyces iridis*	11.00	1.41	31.46	8.42	0.82	0.82	13.66	0.10	0.06	trace	5.32	26.94
32548	*Plectospira myriandra*	4.96	0.48	12.40	2.08	0.39	0.24	7.39	0.07	0.04	0.01	4.87	67.07
32710	*Saprolegnia diclina*	15.32	4.42	17.22	5.06	3.21	1.79	23.27	0.47	0.99	0.64	12.26	15.36
102130	*Thraustotheca clavata*	20.86	6.21	21.76	10.02	1.15	2.43	20.42	0.51	0.49	0.32	2.95	12.87
102547	*Achlya diffusa*	25.64	6.21	29.04	7.22	trace	8.59	9.13	0.51	0.04	0.04	3.04	10.54
104173	*Brevilegnia variabilis*	32.40	3.46	11.92	7.17	0.95	4.54	23.51	0.68	0.02	0.06	2.32	12.98
104176	*Saprolegnia subterranea*	20.39	6.14	9.99	12.15	0.65	3.05	17.30	0.84	trace	0.11	8.75	20.64
104178	*Dictyuchus sterilis*	25.24	11.33	20.81	10.58	0.96	3.21	12.69	1.87	trace	0.06	2.66	10.59

Abbreviations: 16:0, palmitic acid; 18:0, stearic acid; OA, oleic acid; LA, linoleic acid; GLA, γ-linolenic acid; DGLA, dihomo-γ-linolenic acid; ARA, arachidonic acid; ALA, α-linolenic acid; SDA, stearidonic acid; ETA, ω3 eicosatetraenoic acid; EPA, ω3 eicosapentaenoic acid.

[a] Trace refers to values below 0.01

A comparison of the EPA/ARA ratios of all strains showing sufficient growth revealed that *P. sulcatum* (NBRC 100117) and *P. myriandra* (NBRC 32548) had the highest ratios (4.75 and 0.66, respectively) in their respective orders (**Table 1.3**). These two strains also had the highest ω3/ω6 fatty acid ratios in their respective orders. In order to elucidate their ω3 desaturase substrate specificity, the author attempted to isolate ω3 desaturase genes from these two strains.

Table 1.3. EPA/ARA and ω3/ω6 fatty acid ratios of strains showing sufficient growth in GY medium (strains selected for analysis are highlighted)

NBRC no.	Order	Strain	EPA/ARA	ω3/ω6
30346	Peronosporales	*Pythium irregulare*	1.18	0.36
32219	Peronosporales	*Pythium aristosporum*	1.09	0.62
33107	Peronosporales	*Pythium aphanidermatum*	1.31	0.60
100117	Peronosporales	*Pythium sulcatum*	4.75	0.83
100120	Peronosporales	*Pythium torulosum*	1.73	0.57
100125	Peronosporales	*Pythium ultimum*	1.03	0.34
103118	Peronosporales	*Pythium catenulatum*	1.29	0.47
32326	Peronosporales	*Phytophthora cryptogea*	1.74	0.52
31624	Peronosporales	*Phytophthora megasperma*	1.12	0.35
33180	Peronosporales	*Phytophthora cinnamomi*	0.32	0.23
31935	Saprolegniales	*Aphanomyces iridis*	0.39	0.23
32548	Saprolegniales	*Plectospira myriandra*	0.66	0.49
32710	Saprolegniales	*Saprolegnia diclina*	0.53	0.43
102130	Saprolegniales	*Thraustotheca clavata*	0.14	0.13
102547	Saprolegniales	*Achlya diffusa*	0.33	0.15
104173	Saprolegniales	*Brevilegnia variabilis*	0.10	0.08
104176	Saprolegniales	*Saprolegnia subterranea*	0.51	0.29
104178	Saprolegniales	*Dictyuchus sterilis*	0.21	0.17

Cloning of the genes encoding the enzymes involved in EPA synthesis in *P. sulcatum* and *P. myriandra* was achieved by PCR amplification of partial DNA fragments, followed by bidirectional genome walking through inverse PCR as described in “Materials and Methods”. Comparisons of the fragment sequences to cDNA sequences led to the identification of a 1098 bp coding sequence fragment from *P. sulcatum* designated *psulω3* (Accession no. LC589688), a 1068 bp coding sequence fragment from *P. myriandra* designated *pmd17c*, and a 1068 bp coding sequence fragment from *P. myriandra* designated *pmd17g*. *pmd17c* was amplified

using cDNA as a template (Accession no. LC589689) and *pmd17g* was identified as a putative exon sequence based on the genomic sequence (Accession no. LC589690).

Amino acid sequence analysis of PSULω3, PMD17C, and PMD17G

Amino acid sequences of all three isolated genes contained three histidine boxes (**Figure 1.2**, red boxes) and membrane topology analysis by CCTOP (**Figure 1.3**) predicted that all three sequences possessed the four transmembrane domains characteristic of ω3 desaturases. Comparisons to sequences in the NCBI database revealed that PSULω3 showed 81% similarity to a *P. aphanidermatum* fatty acid desaturase, 61% similarity to a *Phytophthora infestans* fatty acid desaturase, and 56% similarity to the *S. diclina* ω3 fatty acid desaturase SDD17. PMD17C and PMD17G both showed 69% similarity to *S. diclina* SDD17, 59% similarity to a *P. aphanidermatum* fatty acid desaturase, and 61% similarity to a *P. infestans* fatty acid desaturase. PMD17C and PMD17G showed 92% similarity to an *Aphanomyces euteiches* hypothetical protein and 80% similarity to a *Thraustotheca clavate* ω3 fatty acid desaturase. PMD17C and PMD17G had 98% sequence similarity, differing by only four amino acid residues.

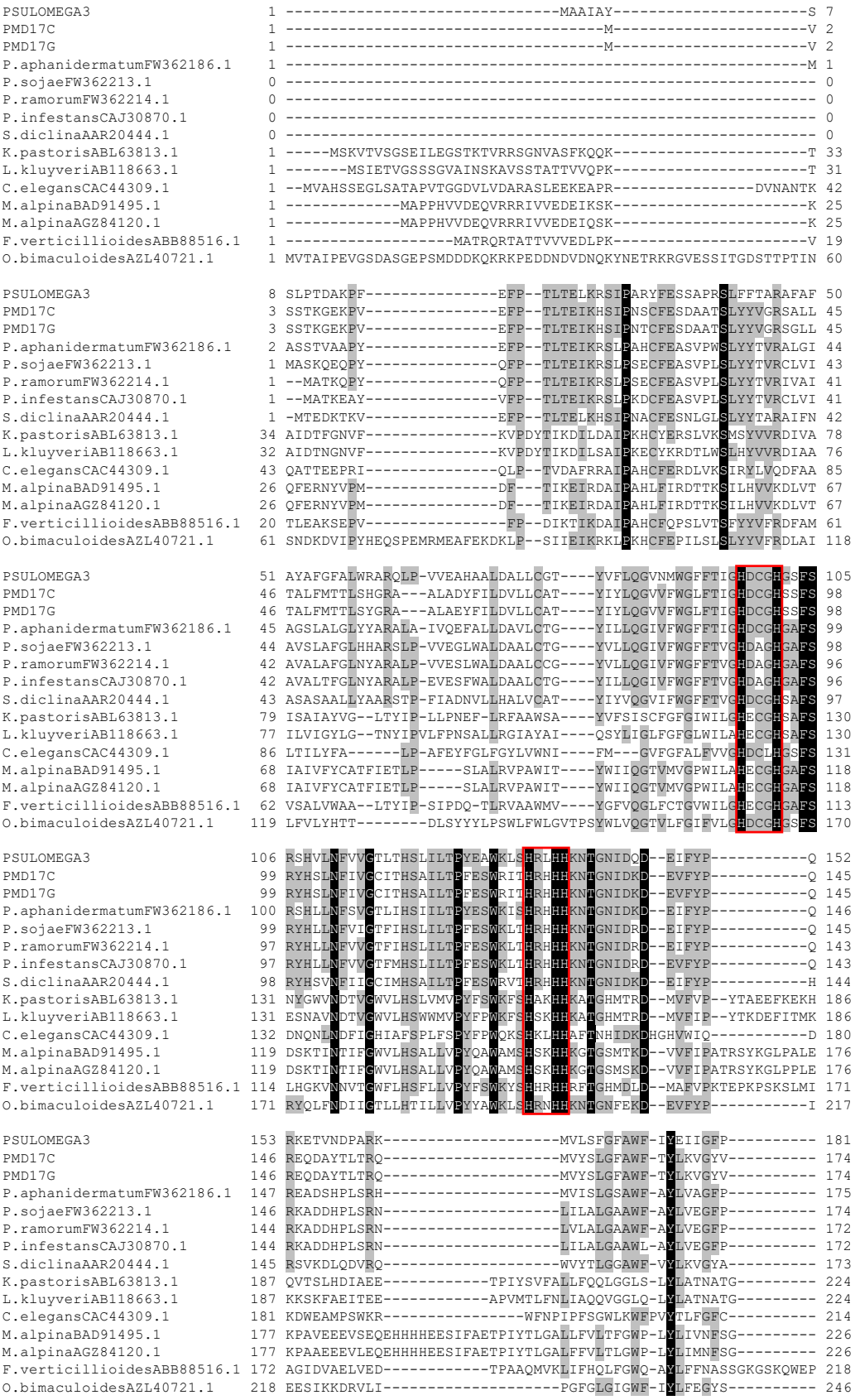
PSULOMEGA3
PMD17C
PMD17G
P.aphanidermatumFW362186.1
P.sojaeFW362213.1
P.ramorumFW362214.1
P.infestansCAJ30870.1
S.diclinaAAR20444.1
K.pastorisABL63813.1
L.kluyveriAB118663.1
C.elegansCAC44309.1
M.alpinaBAD91495.1
M.alpinaAGZ84120.1
F.verticillioidesABB88516.1
O.bimaculoidesAZL40721.1

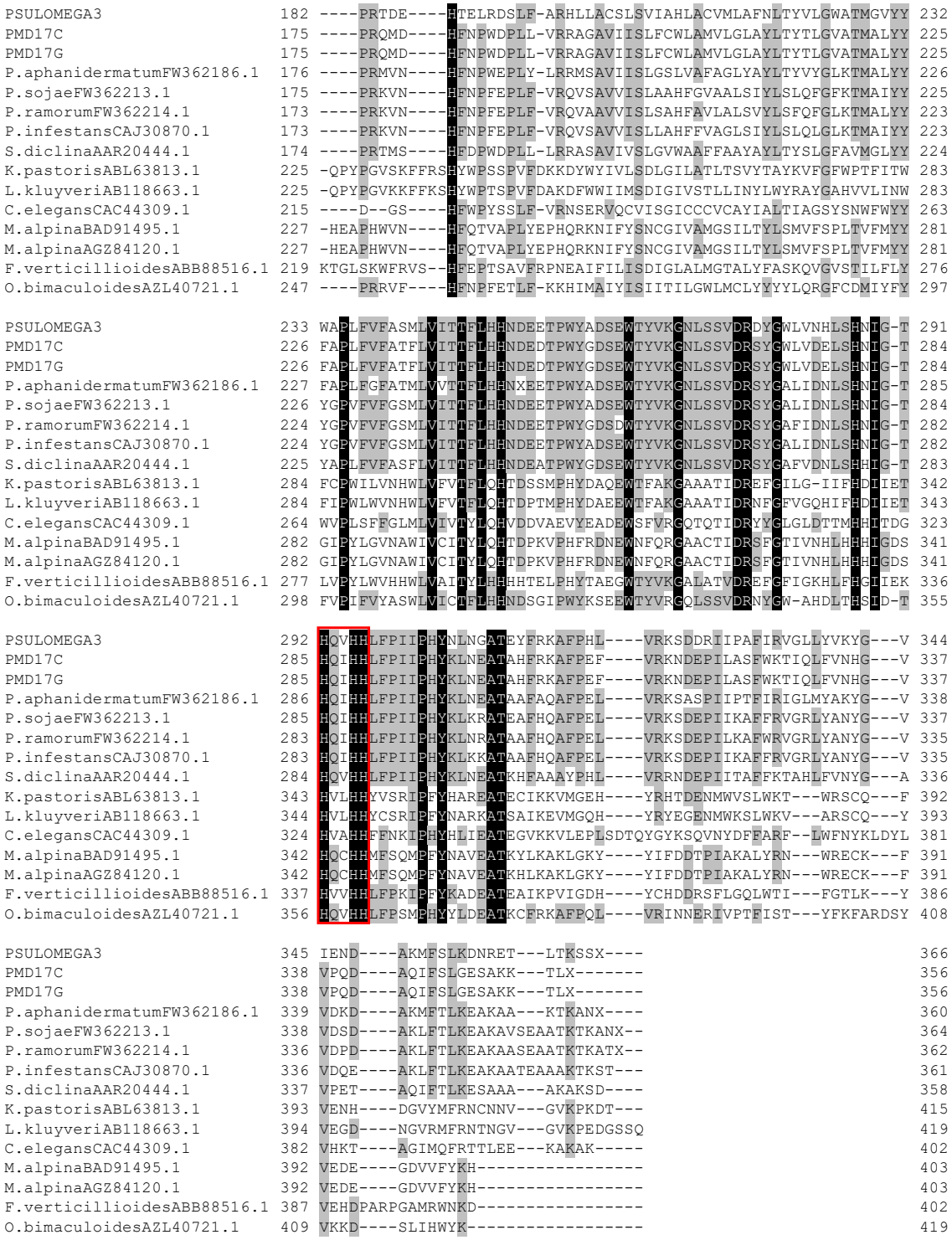

Figure 1.2. Multiple sequence alignment of PSULω3, PMD17C, PMD17G, and notable ω3 fatty acid desaturase amino acid sequences. The three histidine boxes are outlined in red. PSULOMEGA3, *Pythium sulcatum* PSULω3; PMD17C, *Plectospira myriandra* PMD17C; PMD17G, *Plectospira myriandra* PMD17G.

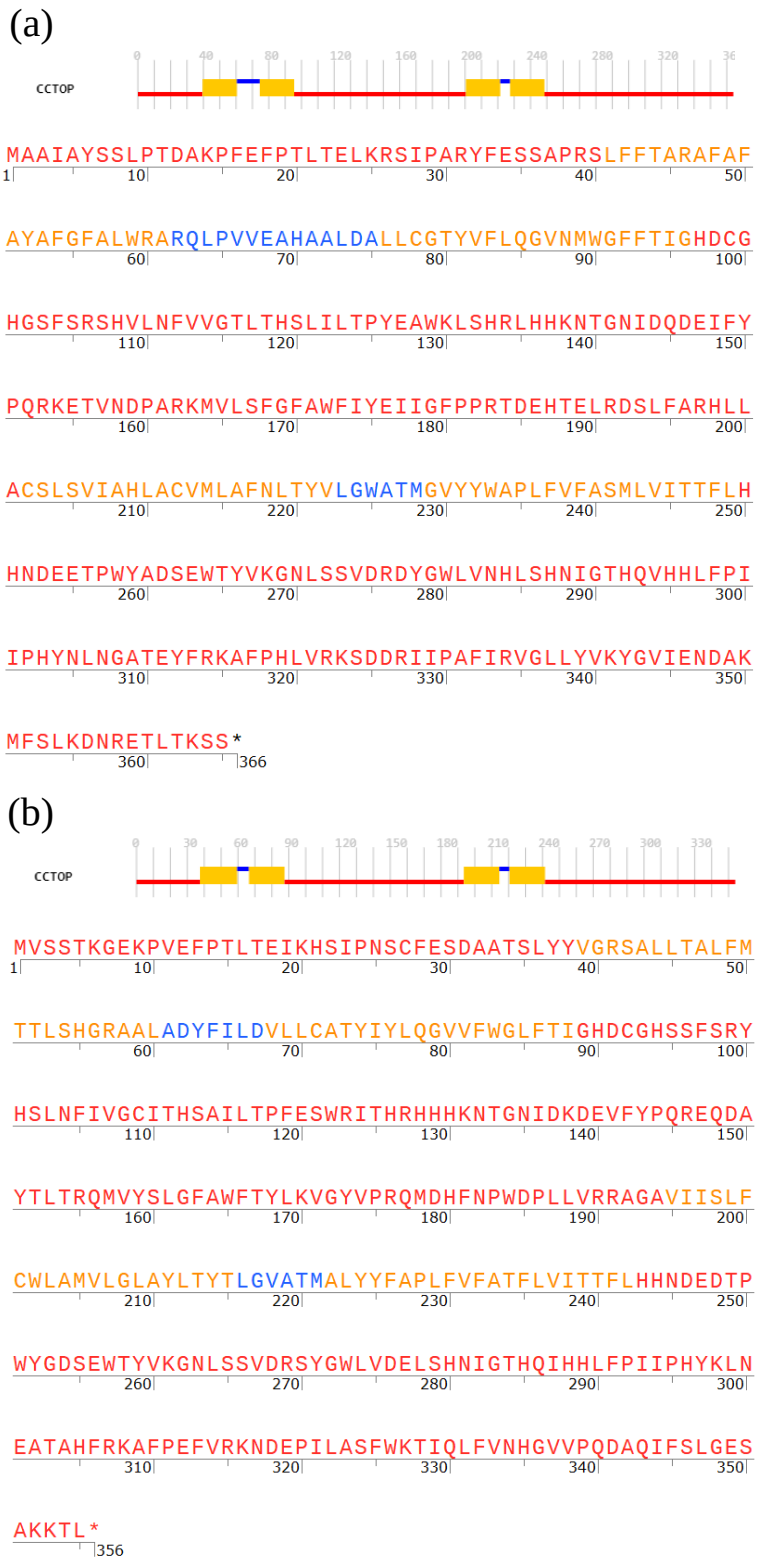

Figure 1.3. Consensus topology predictions generated using CCTOP. (a) PSULω3. (b) PMD17C. (c) PMD17G. Red, intracellular; Yellow, transmembrane; Blue, extracellular.

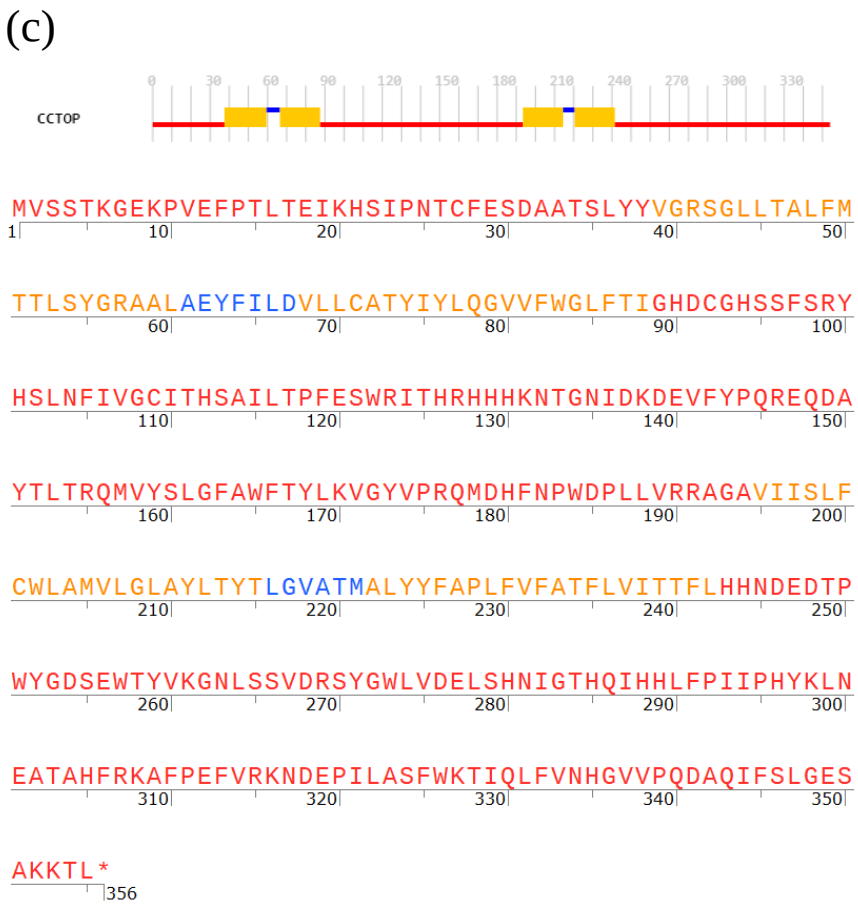

Figure 1.3. Consensus topology predictions generated using CCTOP. (a) PSULω3. (b) PMD17C. (c) PMD17G. Red, intracellular; Yellow, transmembrane; Blue, extracellular.

Phylogenetic analysis of PSULω3, PMD17C, and PMD17G

Phylogenetic analysis of PSULω3, PMD17C, PMD17G, and several known ω3 desaturases (**Figure 1.4**) showed that all three sequences belong to a deep-rooted clade containing all known oomycete ω3 desaturases that are distinct from the branches of ω3 desaturases from animals (*Caenorhabditis elegans*, *Octopus bimaculoides*) and fungi (*M. alpina*, *Fusarium verticillioides*, *Komagataella pastoris, and Lachancea kluyveri*). In the oomycete clade, PSULω3 grouped to a branch distinct from the main branch containing PMD17C, PMD17G, and ω3 desaturases from *S. diclina* and *P. aphanidermatum.* This main branch contains two sub-branches, one of which contains PMD17C, PMD17G, and *S. diclina* ω3 desaturase and the other containing all remaining *Pythium* desaturases.

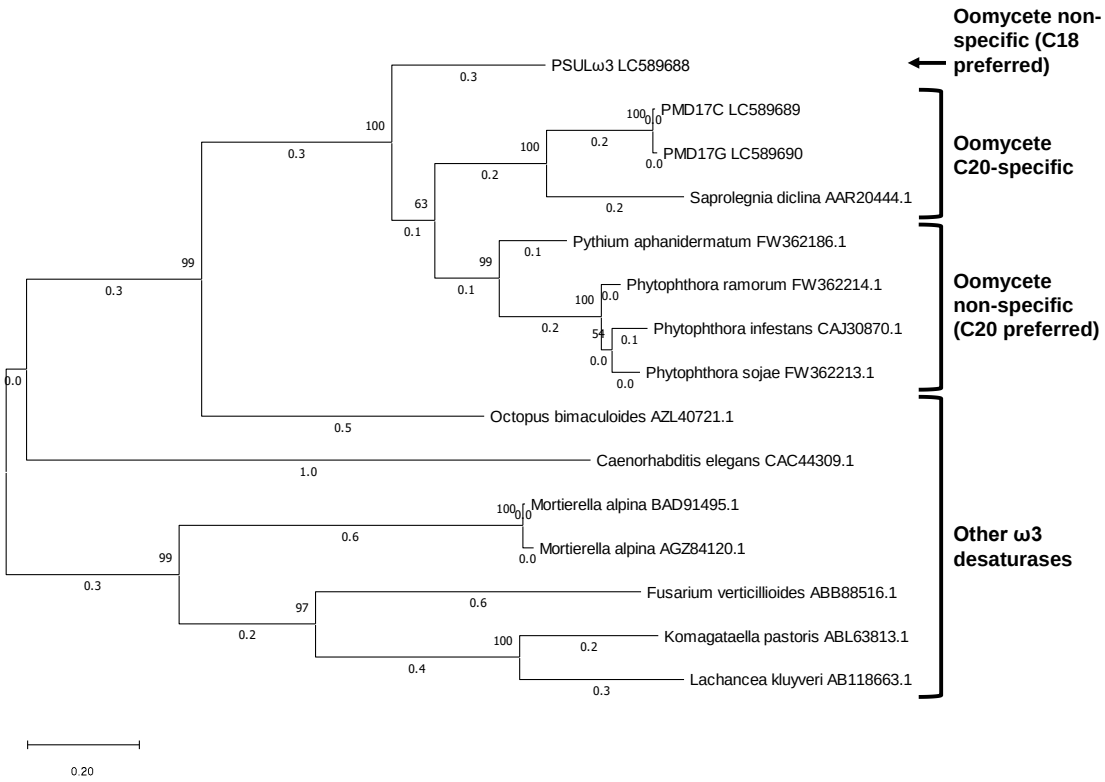

Figure 1.4. Phylogenetic tree of notable ω3 fatty acid desaturases. The tree is drawn to scale, with branch lengths measured in the number of substitutions per site, which are noted next to the branches. PSULω3, *Pythium sulcatum* PSULω3; PMD17C, *Plectospira myriandra* PMD17C; PMD17G, *Plectospira myriandra* PMD17G.

Characterization of putative ω3 desaturases PSULω3, PMD17C, and PMD17G using *Saccharomyces cerevisiae*

Each putative ω3 desaturase was next introduced to the yeast *Saccharomyces cerevisiae* InvSc1 to characterize their function and confirm ω3 desaturase activity. Expression plasmid vectors containing either *psulω3, pmd17c*, or *pmd17g* were constructed (**Figure 1.5**) then introduced into the tryptophan-auxotrophic *S. cerevisiae* strain InvSc1 via electroporation. Isolated transformants were then cultivated in growth medium containing the ω6 fatty acids linoleic acid (LA, 18:2ω6), γ-linolenic acid (GLA, 18:3ω6), dihomo-γ-linolenic acid (DGLA, 20:3ω6), and ARA to characterize ω3 desaturase substrate specificity. *Psulω3* transformants exhibited ω3 desaturase activity on C18 and C20 ω6 PUFAs, converting exogenous LA, GLA, DGLA, and ARA into ALA, SDA, eicosatetraenoic acid (ETA, 20:4ω3), and EPA, respectively.

In contrast, the ω3 desaturases *pmd17c* and *pmd17g* transformants only showed activity on the C20 PUFAs DGLA and ARA (**Figure 1.1**, **Table 1.4**). These results indicate that *psulω3* exhibits ω3 desaturase activity irrespective of carbon chain length, while *pmd17c* and *pmd17g* exhibit ω3 desaturase activity specifically on C20 ω6 PUFAs. Out of the four tested ω6 PUFAs, the *psulω3* transformants converted GLA most efficiently, reaching a conversion rate of 49%, while *pmd17c* and *pmd17g* transformants showed highest desaturase activity for the ARA to EPA reaction, reaching conversion rates of 45% and 33%, respectively (**Table 1.4**).

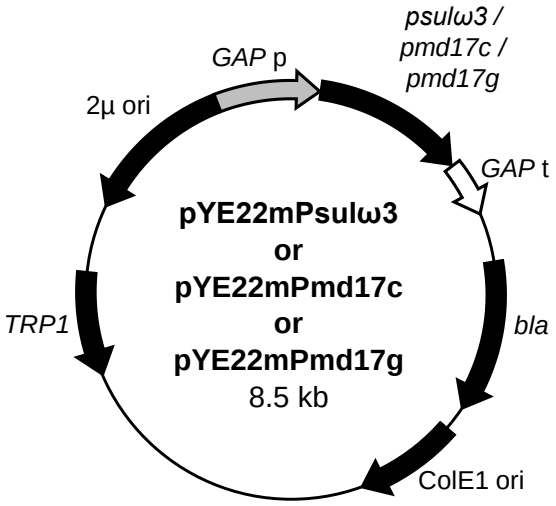

Figure 1.5. Diagram of constructed *S. cerevisiae* expression plasmid vectors. *GAP* p, *GAP* promoter; *GAP* t, *GAP* terminator; *TRP* 1, phosphoribosylanthranilate isomerase *TRP1* gene; *bla*, ampicillin resistance protein gene; ColE1 ori, ColE1 origin of replication; 2µ ori, 2µ origin of replication.

Table 1.4. ω3 Desaturase conversion rate of *psulω3*, *pmd17c*, and *pmd17g* in *S. cerevisiae* transformants

Substrate	Product	Conversion rate (%)[a]		
		PSULω3	PMD17C	PMD17G
LA (18:2ω6)	ALA (18:3ω3)	12.33	0	0
GLA (18:3ω6)	SDA (18:4ω3)	49.38	0	0
DGLA (20:3ω6)	ETA (20:4ω3)	33.29	31.24	22.99
ARA (20:4ω6)	EPA (20:5ω3)	34.19	44.53	33.05

[a]Conversion rate (%) = 100 × (product/[product + substrate])

Evaluation of EPA production via introduction of the ω3 desaturase genes *psulω3, pmd17c,* and *pmd17g* in *Mortierella alpina* under ordinary temperatures

To evaluate the capability of the cloned ω3 desaturases to synthesize EPA under ordinary temperatures (28 °C) in fungi, the ω3 desaturase-encoding genes were introduced into the ARA-accumulating fungus *M. alpina* 1S-4. As *M. alpina* can accumulate ω6-PUFAs to approximately 70% of the TFA content (25), the author thus attempted to convert this ω6 PUFA pool to EPA via ω3 desaturase gene overexpression. To increase heterologous gene expression levels in *M. alpina*, expression plasmid vectors were constructed that contained codon-optimized coding sequences driven by the strong constitutive *SSA2* promoter (32) (**Figure 1.6**). The author then transformed *M. alpina* 1S-4 with the constructed plasmid vectors via *Agrobacterium tumefaciens*-mediated transformation (ATMT) (30) and obtained 34 *psulω3* transformants, 47 *pmd17c* transformants, and 36 *pmd17g* transformants.

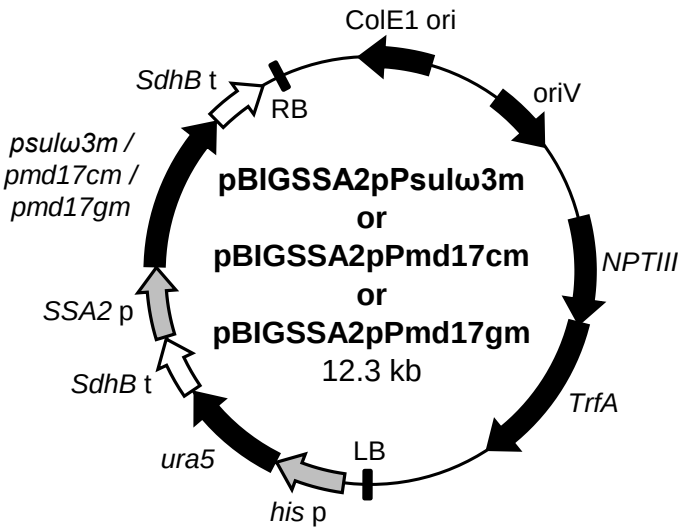

Figure 1.6. Diagram of constructed *M. alpina* expression plasmid vectors. *SSA2* p, *M. alpina SSA*2 promoter; *his* p, *M. alpina* histone H4.1 promoter short fragment; *SdhB* t, *M. alpina SdhB* transcription terminator; *ura5*, orotate phosphoribosyl transferase gene of *M. alpina*; *NPTIII*, neomycin phosphotransferase III gene; *TrfA*, TrfA locus, which produces two proteins that promote plasmid replication; ColE1 ori, ColE1 origin of replication; oriV, pRK2 origin of replication; RB, right border; LB, left border.

For preliminary screening, all transformants were incubated in growth medium for 7 days at 28 °C. The transformants exhibited a high variability of EPA productivity due to random location single copy chromosomal integration (30) (**Figures 1.7a and 1.8a**). In agreement with the C18 and C20 ω6 PUFA substrate specificity of *psulω3* demonstrated in *S. cerevisiae*, most *M. alpina psulω3* transformants accumulated the C18 and C20 ω3 fatty acids ALA, SDA, ETA, and EPA (**Figure 1.7a**). EPA production ranged from 161 to 540 mg L^{-1} (**Figure 1.7b**), and the top EPA producer PS#24 was selected for further analysis.

Both *pmd17c* and *pmd17g* showed strict C20 ω6 PUFA substrate specificity in *S. cerevisiae*. *pmd17c* and *pmd17g M. alpina* transformants mainly accumulated EPA (0%-32% TFAs), produced small amounts of ETA (0%-2% TFAs), and did not accumulate either C18 fatty acids ALA or SDA (**Figure 1.8a**). Total EPA titers ranged from 7.2 to 868 mg L^{-1} (**Figure 1.8b**). The top two EPA producers containing *pmd17c* (C#14 and C#16) and *pmd17g* (G#18 and G#22) were selected for further analysis.

Fatty acid composition and productivity of promising *M. alpina* transformants for EPA production at 28 °C

Transformants showing high EPA production in earlier experiments (PS#24, C#14, C#16, G#18, and G#22), wild-type *M. alpina* 1S-4, and an *S. diclina* transformant containing *sdd17m* driven by the *SSA2* promoter (Sdd#9) were incubated in 20 mL shake flasks at 28 °C for three, seven, or 10 days. For all *M. alpina* transformants, the proportion of EPA constantly increased during the cultivation period (**Figure 1.9a**). The *pmd17g* transformant G#18 had the highest EPA ratio out of all transformants after both 7 days and 10 days. The proportion of EPA/TFAs reached 31% at 7 days and 40% at 10 days, which were both higher than amounts produced by Sdd#9. The fatty acid content of all the transformants was comparable to that of wild-type *M. alpina* 1S-4 after 7 days, but subsequently dropped by around 10% after 10 days, likely due to a lack of glucose feeding into the growth media (**Figure 1.9b**). The most outstanding transformant was G#18, whose TFA content reached 1397 mg L^{-1} and EPA content reached 553 mg L^{-1} after 10 days (**Figure 1.9b**).

(a)

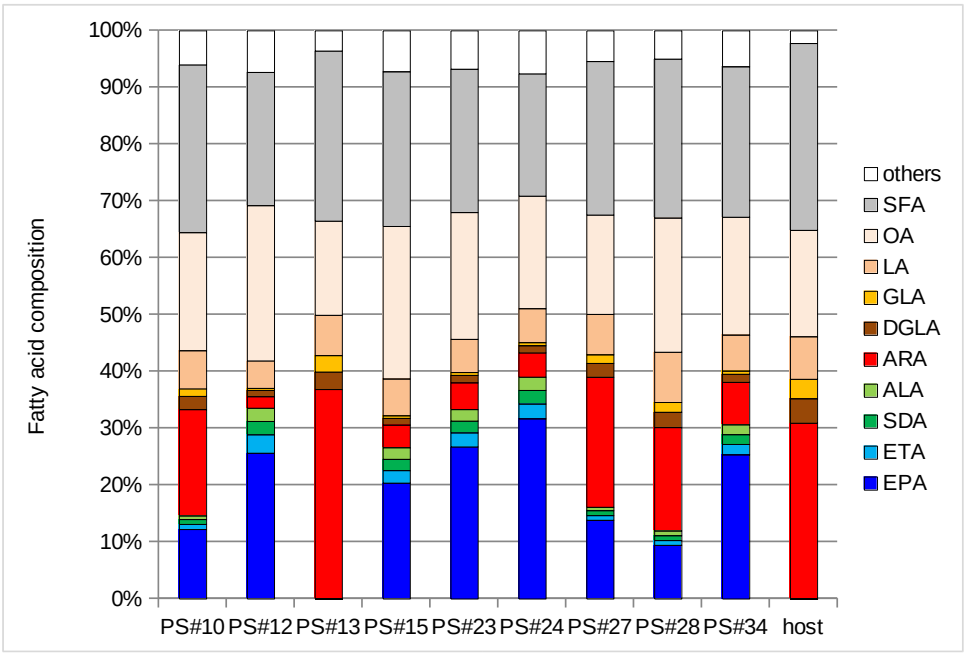

(b)

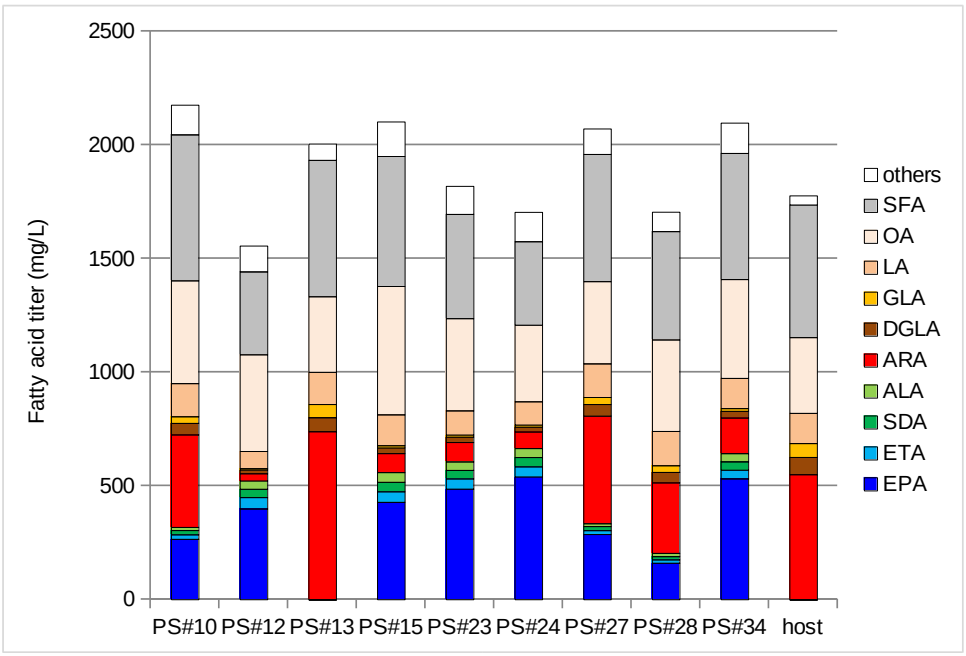

Figure 1.7. (a) Fatty acid composition of and (b) production by the *M. alpina* host strain and its transformants expressing *psulω3m*. All strains were cultivated in 5 mL of GY liquid medium for 7 days at 28 °C. SFA, saturated fatty acids; OA, oleic acid; LA, linoleic acid; GLA, γ-linolenic acid; DGLA, dihomo-γ-linolenic acid; ARA, arachidonic acid; ALA, α-linolenic acid; SDA, stearidonic acid; ETA, ω3 eicosatetraenoic acid; EPA, ω3 eicosapentaenoic acid.

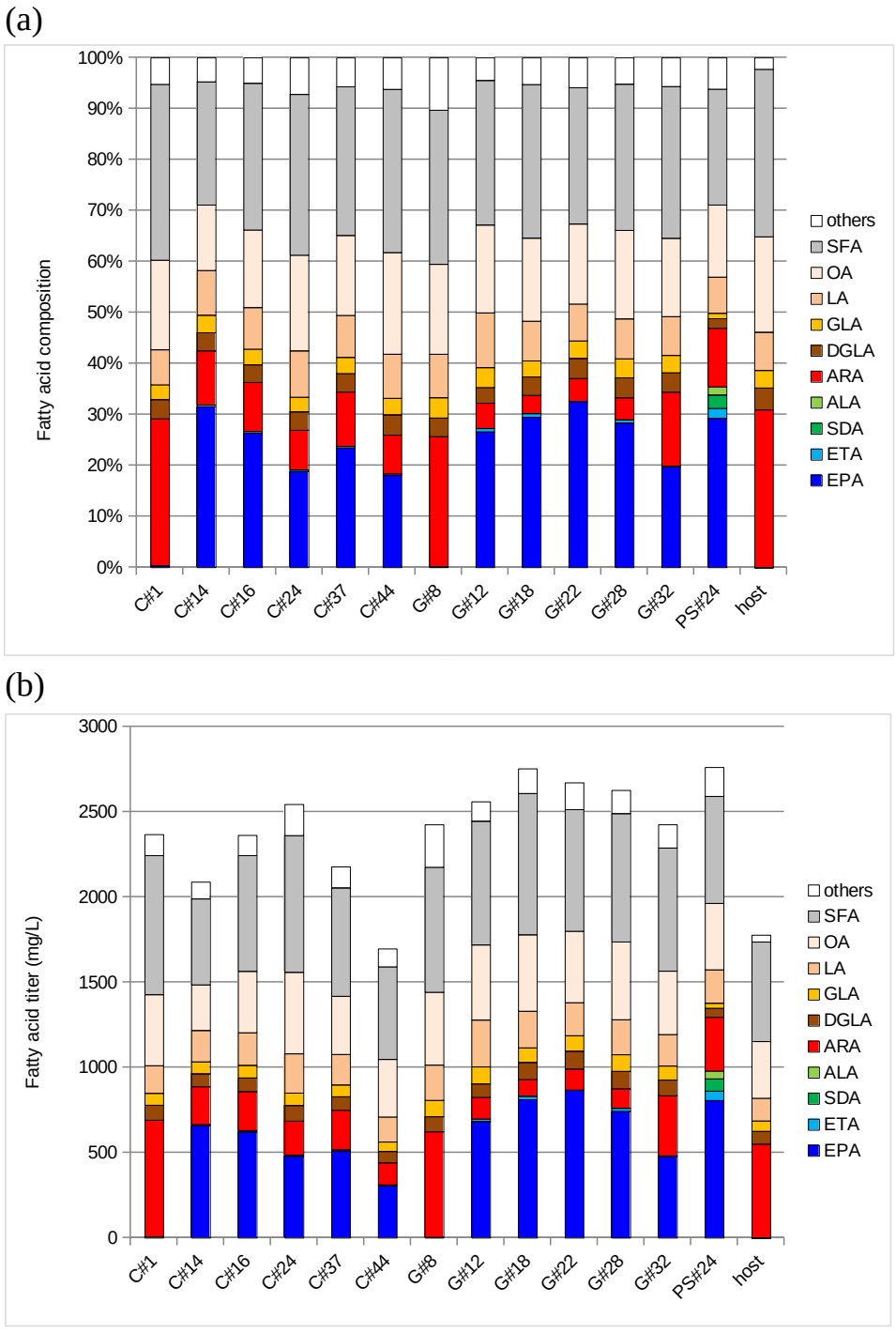

Figure 1.8. (a) Fatty acid composition of and (b) production by the *M. alpina* host strain and its transformants expressing *pmd17cm* (C#1, C#14, C#16, C#24, C#37, and C#44) and *pmd17gm* (G#12, G#18, G#22, G#28, and G#32). All strains were cultivated in 5 mL of GY liquid medium for 7 days at 28 °C. SFA, saturated fatty acids; OA, oleic acid; LA, linoleic acid; GLA, γ-linolenic acid; DGLA, dihomo-γ-linolenic acid; ARA, arachidonic acid; ALA, α-linolenic acid; SDA, stearidonic acid; ETA, ω3 eicosatetraenoic acid; EPA, ω3 eicosapentaenoic acid.

(a)

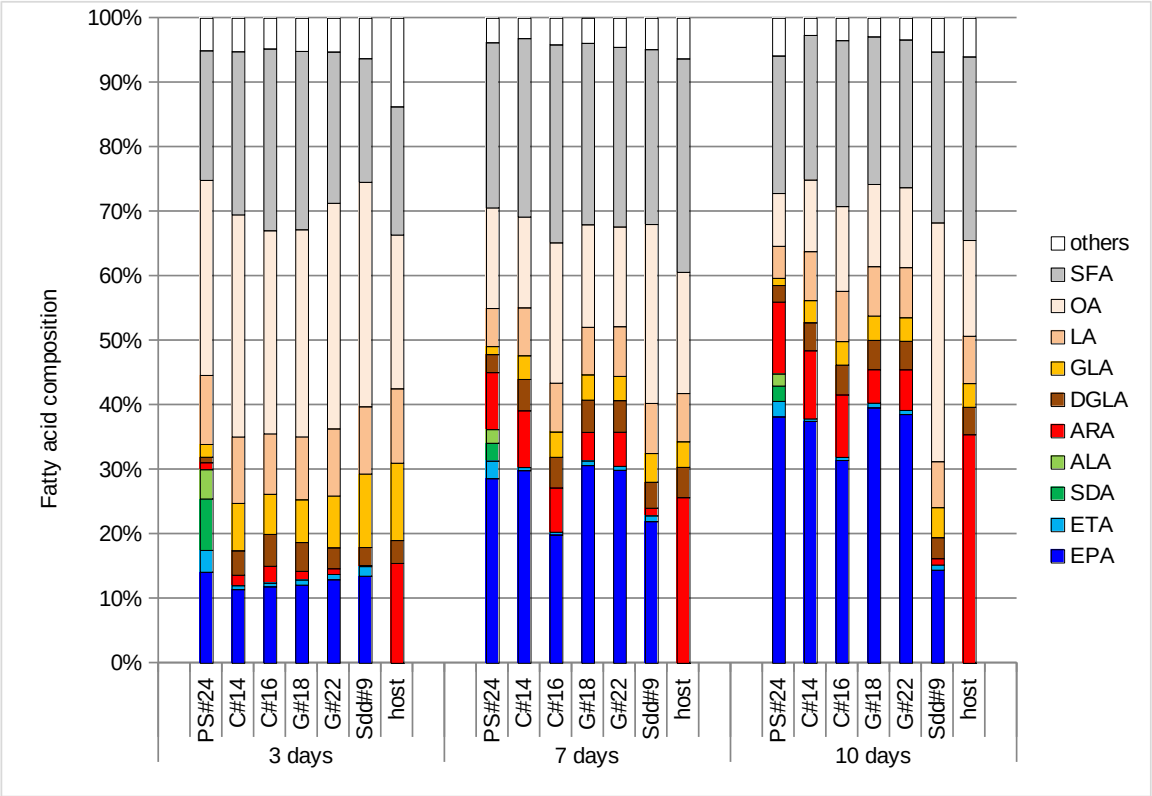

Figure 1.9. (a) Fatty acid composition of the *M. alpina* host strain and selected transformants expressing *psulω3m* (PS#24), *pmd17cm* (C#14 and C#16), *pmd17gm* (G#18 and C#22), and *sdd17m* (Sdd#9). All strains were cultivated in 4 mL of GY liquid medium for 3, 7, or 10 days at 28 °C. SFA, saturated fatty acids; OA, oleic acid; LA, linoleic acid; GLA, γ-linolenic acid; DGLA, dihomo-γ-linolenic acid; ARA, arachidonic acid; ALA, α-linolenic acid; SDA, stearidonic acid; ETA, ω3 eicosatetraenoic acid; EPA, ω3 eicosapentaenoic acid.

(b)

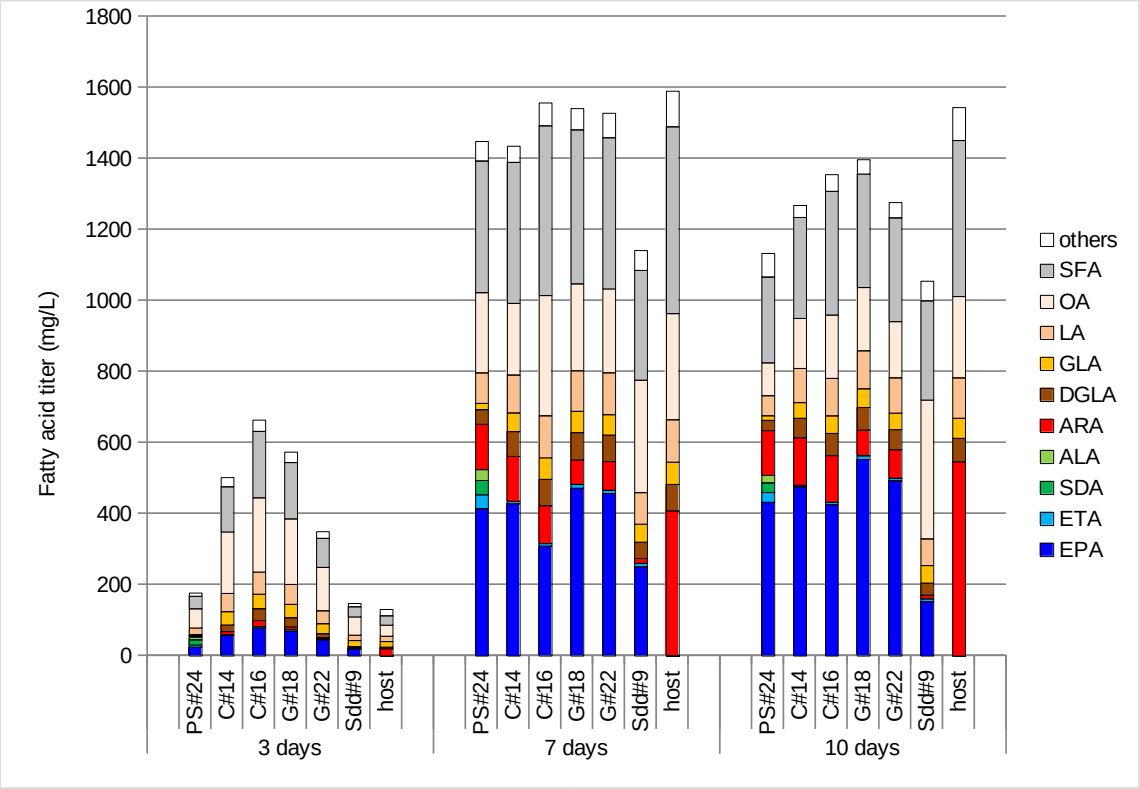

Figure 1.9. (b) production by of the *M. alpina* host strain and selected transformants expressing *psulω3m* (PS#24), *pmd17cm* (C#14 and C#16), *pmd17gm* (G#18 and C#22), and *sdd17m* (Sdd#9). All strains were cultivated in 4 mL of GY liquid medium for 3, 7, or 10 days at 28 °C. SFA, saturated fatty acids; OA, oleic acid; LA, linoleic acid; GLA, γ-linolenic acid; DGLA, dihomo-γ-linolenic acid; ARA, arachidonic acid; ALA, α-linolenic acid; SDA, stearidonic acid; ETA, ω3 eicosatetraenoic acid; EPA, ω3 eicosapentaenoic acid.

DISCUSSION

Non-specific and C20-specific ω3 desaturases with efficient desaturase activity are vital for EPA production regardless of the targeted pathway (**Figure 1.1**). However, reports of such genes, and strategies to screen such gene resources have been limited to date. In this study, the author devised a method of selecting oomycetes with efficient ω3 desaturases based on intracellular EPA/ARA ratios, and demonstrated the viability of this strategy through the discovery of a non-specific ω3 desaturase gene from *P. sulcatum* (NBRC 100117), *psulω3,* as well as two C20-specific ω3 desaturase genes from *P. myriandra* (NBRC 32548), *pmd17c* and *pmd17g*. The feasibility of utilizing these enzymes for EPA production was evaluated by expression in *M. alpina*.

Oomycetes are known PUFA producers and are thought to use the desaturase/elongase pathway based on lipid profiles and known enzymes (18–21). The fatty acid profiles produced during screening (**Table 1.2**) showed that some species such as *P. sulcatum* produced all ω3 fatty acids while others such as *P. myriandra* did not produce significant levels of any ω3 fatty acids apart from EPA. This strongly suggests that an ω3 desaturase recognizing C18 and possibly C20 substrates is present in the former group, while an ω3 desaturase recognizing only C20 substrates is characteristic of species in the latter group. The author then predicted that the EPA/ARA ratio would be a good approximate indication of ω3 desaturases activity useful for EPA production. Using this strategy, the two species with the highest EPA/ARA ratios in their respective orders were selected, *P. sulcatum* (Peronosporales) and *P. myriandra* (Saprolegniales). Both species exhibited superior EPA/ARA ratios compared to other strains from the same orders with known ω3 desaturases, *P. aphanidermatum* (Peronosporales) and *S. diclina* (Saprolegniales), suggesting higher ω3 desaturase activity (**Table 1.3**). *P. sulcatum and P. myriandra* also showed the highest ω3/ω6 fatty acid ratios in their respective orders, suggesting that overall ω6 to ω3 fatty acid flux was highest in these two strains. Since these strains were discovered after only briefly screening several strains, it is expecte that even more ω3 desaturase genes could be discovered via a broader search of oomycetes and other species with similar lipid profiles.

The three new identified desaturase genes, *psulω3* from *P. sulcatum* and *pmd17c* and *pmd17g* from *P. myriandra*, coded for ω3 desaturases that had varying specificity toward C18 and C20 fatty acids (**Table 1.4**). Characterization of enzyme activity in *S. cerevisiae* showed

that PSULω3 catalyzed addition of an ω3 double bond to C18 and C20 fatty acids and exhibited the highest preference for GLA, followed by ARA, DGLA, and LA (**Figure 1.1**, **Table 1.4**). This indicated that PSULω3 is a non-specific ω3 desaturase that has major activity on C18 fatty acids and minor activity on C20 fatty acids. Interestingly, PSULω3 exhibited similar substrate ranges but different substrate preferences to the three Peronosporales ω3 desaturases described in a previous study (42). While PSULω3 most favored GLA, enzymes characterized in the previous study most preferred ARA, with lower activity using DGLA and the least activity with GLA. In *psulω3* transformants, such high conversion efficiency of GLA to SDA (49%) was unexpected, as *P. sulcatum* only produced 1.7% SDA/TFA (although this represents the highest SDA/TFA value of all screened Peronosporales strains) (**Table 1.2**). This suggests that a highly efficient elongase and Δ5 desaturase of the ω3 pathway toward EPA are present in *P. sulcatum* and may be underlying factors in its high EPA/ARA ratio.

In contrast to PSULω3, PMD17C and PMD17G only catalyzed the addition of ω3 double bonds for C20 fatty acids, with strongest substrate preference for ARA and moderate preference for DGLA. PMD17C and PMD17G are thus C20-specific ω3 desaturases, similar to the only previously known C20-specific ω3 desaturase *S. diclina* SDD17 (40). Comparison of their conversion efficiencies indicated that the DGLA and ARA conversion rates of PMD17C (31% and 44%) and PMD17G (23% and 33%) were substantially higher than those of SDD17 (5% and 26%). However, it is unknown how factors such as protein expression levels and cultivation conditions affect this comparison. Amino acid sequence alignment and desaturation substrate activity analysis showed that the two *P. myriandra* enzymes were highly homologous (98% similarity) and had similar substrate preferences (**Table 1.4**), suggesting that *pmd17c* and *pmd17g* are isozymes originating from a single gene. Interestingly, while both genes were amplified from genomic DNA, only *pmd17c* was successfully amplified from cDNA reverse-transcribed from total RNA. This means *pmd17g* is either not expressed or is expressed at a lower level than *pmd17c*, possibly due to accumulated mutations in regulatory sequences. It is not clear whether PMD17G actively catalyzes desaturation in *P. myriandra*.

PSULω3, PMD17C, and PMD17G shared all the conserved features previously reported for oomycete ω3 desaturases (34, 40, 42). ω3 Desaturases are membrane bound proteins characterized by the presence of three histidine boxes, ($HX_{3-4}H$, $HX_{2-3}HH$, and $H/QX_{2-3}HH$) and usually have 4-6 membrane spanning helices that account for ~1/3 of their amino acid sequences (44). Sequence comparisons revealed that PSULω3, PMD17C, and

PMD17G all contained three histidine boxes (**Figure 1.2**, red boxes), as well as two extended hydrophobic stretches of amino acid residues predicted to be transmembrane domains based on CCTOP membrane topology analysis (**Figure 1.3**). Like other ω3 desaturases, PSULω3, PMD17C, and PMD17G contained C-terminal lysine residues (K-3, K-4+K-3, and K-4+K-3, respectively) associated with the retention of transmembrane proteins in the endoplasmic reticulum (45). In addition, all three enzymes also lacked an N-terminal cytochrome b_5 heme-binding domain (46), meaning they are not fusion desaturases and probably receive electrons from microsomal cytochrome b_5. Interestingly, comparisons of conserved sequence motifs in PSULω3, PMD17C, and PMD17G reveal the presence of a glutamine residue in the second position of the third conserved histidine motif, while a valine residue is typically observed in that position for most ω3 desaturases identified to date (47). This difference may contribute to the C20 fatty acid activity observed for certain ω3 desaturases, since a previous report showed that the sequences in histidine boxes play a pivotal role in determining desaturase substrate preference (48), although a previous mutagenic study did not examine this residue (49).

Phylogenetic analysis (**Figure 1.4**) clarifies the evolutionary relationship of oomycete ω3 desaturases reported to date. From the results, it is inferred that all known oomycete ω3 desaturases evolved separately from ω3 desaturases in fungi and animals, and that oomycete ω3 desaturases possibly evolved from a non-specific ω3 desaturase ancestor shared with *O. bimaculoides* that shares a preference for C20 substrates. In the clade containing all known oomycete ω3 desaturases, *psulω3* then evolved separately from the other oomycete desaturases and obtained mutation(s) conferring a preference for GLA as a desaturation substrate. In a separate branch, an ancestor of *S. diclina* and *P. myriandra* subsequently obtained mutation(s) inhibiting desaturase activity on C18 substrates while an ancestor of the remaining non-specific ω3 desaturases evolved separately. This interpretation is consistent with the theory that both specific and non-specific ω3 desaturases arose from one ancestral ω3 desaturase (47). The authors theory that oomycetes evolved independently is also corroborated by an extensive phylogenetic study which places oomycete desaturases as a sister group to the animal desaturases (50). This study adds to known knowledge by showing that *psulω3* is the closest oomycete ω3 desaturase in evolutionary distance to the ancestral common ω3 desaturase out of all known oomycete ω3 desaturases. Based on the produced phylogenetic tree and lipid profiles of Saprolegniales species, evidence is also shown that suggests

oomycetes of the order Saprolegniales all contain C20-specific ω3 desaturases, and that the desaturases most likely evolved from a common ancestor possessing this trait.

From a biotechnological standpoint, the three isolated enzymes appear to be effective for EPA production via the two strategies previously mentioned (PSULω3 for the optimization of total ω6 to ω3 fatty acid flux toward EPA and PMD17C or PMD17G for targeted conversion of the large C20 ω6 fatty acid pool with minimal C18 byproducts). Expression of these enzymes in *M. alpina* at ordinary temperatures (28 °C) produced the highest EPA/TFA values out of all such values reported to date in *M. alpina*, confirming their capability for EPA bioproduction. Compared to strains expressing *pmd17c* and *pmd17g,* the strain PS#24 expressing *psulω3* showed less accumulation of LA and GLA byproducts as they were presumably converted to the C18 ω3 fatty acids ALA and SDA. While TFA content decreased from days 7 to 10 of growth likely due to glucose depletion, EPA production peaked and reached 433 mg L^{-1}, with EPA comprising 38% of the TFA content (**Figure 1.9**). This ratio is higher than those in reports describing *M. alpina* transformants expressing ω3 desaturases to date (34, 36). These results overall thus show that *psulω3* could be employed for efficient EPA production in organisms with efficient ω6 and ω3 pathways. Alternatively, the overexpression of additional desaturase and elongase genes for higher EPA production may also be possible.

M. alpina expressing *pmd17c* and *pmd17g* accumulated EPA as a major product with a minimal accumulation of other ω3 byproducts, such as ALA and SDA. EPA production by the *pmd17c* expressing strain C#14 peaked at day 10, reaching 475 mg L^{-1} and comprising 38% of TFAs (**Figure 1.9**). Expressing *pmd17g* led to highest EPA production compared to expression of the other two enzymes, contradicting the results of fatty acid feeding experiments in *S. cerevisiae* that suggested that PMD17C had higher activity than PMD17G with ARA. Strain G#18 achieved an EPA titer of 553 mg L^{-1} at day 10, with EPA levels reaching 40% of TFAs (**Figure 1.9**). This represented approximately 3-fold increases in both production metrics compared to the EPA titer and ratio of the strain Sdd#9 expressing *S. diclina sdd17* (152 mg L^{-1} and 14% of TFAs). The EPA/TFA value achieved by G#18 is the highest among those reported to date in *M. alpina*, and is the second highest among currently known EPA sources, with only engineered *Y. lipolytica* producing a higher EPA/TFA ratio (17). These results show that *pmd17c* and *pmd17g* is most suitable for EPA production in *M. alpina* due to its ability to efficiently convert endogenous C20 ω6 fatty acids to their ω3 counterparts with little production of unwanted C18 byproducts.

Despite the progress made, several unanswered questions remain, including why PMD17C exhibited superior substrate conversion efficiency compared to PMD17G in *S. cerevisiae* but not in *M. alpina*. In addition, the lipid class preferences of the three enzymes were not fully examined in this study; while it was suggested that *Phytophthora ramorum* ω3 desaturase most likely prefers phospholipids as substrates (42), more research is needed to determine the lipid affinity of these three enzymes. Mutagenesis studies and crystal structure analyses of these enzymes are also necessary to determine if the glutamine residue in the third histidine box, or other residues, influence the strong ω3 desaturase activity on C20 fatty acids that is characteristic of oomycete ω3 desaturases. Finally, it remains to be seen whether or not the EPA titer and ratio in *M. alpina* can be further increased by methods such as multicopy gene insertion. In *Y. lipolytica*, expressing multiple copies of ω3 desaturase increased the ARA to EPA conversion efficiency from 64% to as much as 95% (17). Further research is needed to determine whether this strategy is feasible in *M. alpina*.

MATERIALS AND METHODS

Organisms and culture conditions

Preliminary screening for ω3 fatty acid production was performed with 35 strains belonging to the orders Peronosporales and Saprolegniales (**Table 1.1**) that were purchased from the National Institute of Technology and Evaluation Biological Resource Center (National Institute of Technology and Evaluation, NITE, Tokyo, Japan). 5 mL of GY medium (2% glucose and 1% Bacto yeast extract) were inoculated with strains transferred directly from slants and cultured strains at 28 °C for 7 days with shaking at 300 strokes min^{-1}.

Enzyme substrate specificity was characterized using *S. cerevisiae* InvSc1 (Thermo Fisher Scientific). The strain was stocked on YPD agar medium (2% glucose, 2% Difco peptone, 1% Difco yeast extract, and 1.5% agar). Yeast transformants were inoculated into test tubes containing 5 mL YPD medium supplemented with adenine (2% glucose, 2% Difco peptone, 1% Difco yeast extract, and 40 mg L^{-1} adenine). The transformants were then precultured at 28 ºC with shaking at 300 strokes min^{-1} for 1 day and 100 µL of resulting preculture was added to test tubes containing 10 mL of YPD supplemented with adenine and various free fatty acids respectively (2% glucose, 2% Difco peptone, 1% Difco yeast extract, 40 mg L^{-1} adenine, 0.1 mM free fatty acids [LA, GLA, DGLA, or ARA], and 0.2% tergitol). Cultures were incubated 28 ºC with shaking at 300 strokes min^{-1} for 2 days.

M. alpina 1S-4 was used for the evaluation of EPA production and was previously isolated from soil near the Kyoto University Graduate School of Agriculture (25). For incoculum preparation, all transformants were first grown on GY agar plates for 4 days. 3mm squares were then excised from the respective plates, inoculated into test tubes containing 5 mL of GY medium (2% glucose and 1% yeast extract) and cultured at 28 °C for 7 days with shaking at 300 strokes min^{-1}. Transformants that showed high growth and fatty acid production were inoculated as previously described into 20 mL Erlenmeyer flasks containing 4 mL of GY medium. The strains were cultured at 28 °C for 3, 7, and 10 days with shaking at 120 strokes min^{-1}.

Genomic DNA extraction and cDNA library construction

For genomic DNA extraction, *P. sulcatum* (NBRC 100117) and *P. myriandra* (NBRC 32548) were inoculated into test tubes containing 10 mL of GY medium and incubated at

28 °C for 7 days with shaking at 300 strokes min^{-1}. The cells were then disrupted with metal corn using a multibead shocker (Yasui Kikai, Osaka, Japan) and genomic DNA extracted using the cetyltrimethylammonium bromide (CTAB) method as described previously (51).

For cDNA library construction, *P. sulcatum* (NBRC 100117) and *P. myriandra* (NBRC 32548) were inoculated into test tubes containing 10 mL of GY medium and incubated at 28 °C for 7 days with shaking at 300 strokes min^{-1}. Total RNA was extracted using ISOGEN (Nippon gene, Toyama, Japan) and transcribed into cDNA using the Prime Script2 High Fidelity RT-PCR Kit (Takara, Shiga, Japan) according to the manufacturer's user manual.

Cloning and sequencing of *psulω3* and *pmd17*

Based on the nucleotide sequences of known ω3 desaturases, two degenerate primers were designed (**Table 1.5**, EPA F-1 and EPA R-1) to amplify partial fragments of the putative genes *psulω3* and *pmd17*. PCR was performed for 35 cycles each consisting of 94 ºC for 1 min, 50 ºC for 1 min and 72 ºC for 1.5 min using Prime STAR GXL (Takara). The resulting 0.6 kb fragments were purified, cloned into a pUC118 plasmid vector using a Blunt End Mighty Cloning Reagent Set (Takara), and sequenced using the GenomeLab DTCS-Quick Start Kit (Beckman Coulter, California, USA).

To amplify full-length gene sequences, four inverse PCR primers were designed for *psulω3* (**Table 1.5**, 100117IPCR F-1, 100117IPCR F-2, 100117IPCR R-1, and 100117IPCR R-2) and *pmd17* (**Table 1.5**, 32548IPCR F-1, 32548IPCR F-2, 32548IPCR R-1 and 32548IPCR R-2) respectively based on the nucleotide sequences of the sequenced fragments. After performing restriction enzyme digestions on *P. sulcatum* genomic DNA with *Kpn*I (Takara) and *P. myriandra* gDNA with *Eco*RV (Takara), inverse PCR was performed for 35 cycles each consisting of 94 ºC for 1 min, 55 ºC for 1 min and 72 ºC for 3 min using Prime STAR GXL (Takara). The resulting 1.1 kb fragments were purified and cloned into a pUC118 plasmid vector using the Blunt End Mighty Cloning Reagent Set (Takara) and sequenced using the GenomeLab DTCS-Quick Start Kit (Beckman Coulter). Coding sequences were determined by comparing the genomic DNA and cDNA sequences.

Table 1.5. Primers used for the amplification of putative ω3 desaturases

EPA F-1	5'- CAYCAYAARAAYACIGGIAAYATHGA -3'
EPA R-1	5'- TGIGGDATDATIGGRAAIARRTGRTG -3'
100117IPCR F-1	5'- CTACGTCAAGGGCAACCTCTCGTCC -3'
100117IPCR F-2	5'- GGATCGCGACTACGGCTGGCTGGTC -3'
100117IPCR R-1	5'- AAAGCCGAACGACAGCACCATCTTG -3'
100117IPCR R-2	5'- CGTCTCTTTGCGCTGCGGGTAAAAG -3'
32548IPCR F-1	5'- ATGGCTTGTTGATGAATTGAGTCAC -3'
32548IPCR F-2	5'- GCAATCTTTCATCTGTGGATCGTTC -3'
32548IPCR R-1	5'- ATACACCATTTGACGAGTTAATGT -3'
32548IPCR R-2	5'- GGTAGGTAAACCAAGCAAATCCAAG -3'

DDBJ accession numbers

Pythium sulcatum psulω3: LC589688; *Plectospira myriandra pmd17c*: LC589689; *Plectospira myriandra pmd17g*: LC589690

***In silico* analysis of amino acid sequences**

Consensus membrane topology predictions of PSULω3, PMD17C, and PMD17G were performed using CCTOP (52).

For multiple sequence alignments, amino acid sequences of chosen ω3 desaturases were acquired from the literature. ω3 Desaturases from *P. aphanidermatum* (42) (FW362186.1), *Phytophthora sojae* (42) (FW362213.1), *P. ramorum* (42) (FW362214.1), *P. infestans* (53) (CAJ30870.1), *S. diclina* (40) (AAR20444.1), *K. pastoris* (41) (ABL63813.1), *L. kluyveri* (38) (AB118663.1), *C. elegans* (37, 54) (CAC44309.1), *M. alpina* (39, 55) (BAD91945.1 and AGZ84120.1), *F. verticillioides* (56) (ABB88516.1), and *O. bimaculoides* (43) (AZL40721.1) were chosen. Multiple sequence alignment was performed using the MUSCLE algorithm (57) with MEGA X version 10.1.8 (58) and default parameters. The multiple sequence alignment was visualized using Genetyx (GENETYX CORPORATION, Japan).

Evolutionary relationship analysis was conducted using MEGA X version 10.1.8 with the amino acid sequences described above. The 15 amino acid sequences were aligned using the MUSCLE algorithm (57) with default parameters. The evolutionary history was inferred using the maximum likelihood method and JTT matrix-based models (59). The tree with the highest log likelihood (-8896.59) is shown. The percentage of trees in which the associated taxa clustered together is shown next to the branches. Initial tree(s) for the heuristic search

were obtained automatically by applying Neighbor-Join and BioNJ algorithms to a matrix of pairwise distances estimated using the JTT model then selecting the topology with the highest log likelihood value. The phylogenetic tree (**Figure 1.4**) is drawn to scale, with branch lengths measured in the number of substitutions per site and listed next to the branches. This analysis involved 15 amino acid sequences and there were a total of 513 positions in the final dataset.

Construction of plasmid vectors for enzyme expression in *S. cerevisiae*

pYE22mPsulω3 and pYE22mPmd17c (**Figure 1.5**) were constructed as follows. pYE22m plasmid vector is a GAP promoter-containing high-expression yeast plasmid vector. *psulω3* gene and *pmd17c* gene fragments were amplified by PCR using full-length fragments derived from cDNA as templates and primers shown in **Table 1.6**. The amplified fragments were digested with either *Eco*RI and *Bam*HI or *Spe*I and *Bgl*II restriction enzyme pairs and cloned into either the *Eco*RI/*Bam*HI-digested pYE22m plasmid vector or the *Nhe*I/*Bam*HI-digested pYE22m plasmid vector, respectively.

Table 1.6. Primers used in PCR for plasmid construction

Gene	Primer	Sequence
Psulω3	PsulYEEcoRI-F	5'- gtgaattcATGGCTGCGATCGCCTATAGCTCGC -3'
	PsulYEBamHI-R	5'- gtggatccCTACGAGCTCTTGGTGAGCGTCTC -3'
*Pmd17*c	PmYESpeI-F	5'- gtactagtATGGTGTCGAGTACAAAGGGG -3'
	PmYEBglII-R	5'- gtagatctTTACAATGTCTTTTTGGCACTTTCAC -3'
*Pmd17*g	SpeI-A-F	5'- gtactagtATGGTGTCGAGTACAAAGGGG -3'
	A-R	5'- AGAAGAGGATCCCAAGGATTAAAGTGATCCATTTGACG -3'
	B-F	5'- ATCACTTTAATCCTTGGGATCCTCTTCTCGTTCGTCG -3'
	B-R	5'- TTCATCATTATGATGCAAGAACGTTGTGATGACCAAAAAC -3'
	C-F	5'- ATCACAACGTTCTTGCATCATAATGATGAAGATACACCATG -3'
	BglII-C-R	5'- gtagatctTTACAATGTCTTTTTGGCACTTTCAC -3'

Restriction sites are underlined. Non-underlined lowercase letters indicate primer overhangs used to facilitate efficient restriction enzyme digestion.

pYE22mPmd17g (**Figure 1.5**) was constructed as follows. Three fragments of putative exon regions of the *pmd17g* gene were amplified by PCR using the *pmd17g* gene fragment with the putative intron region as template and primers shown in **Table 1.6**. The three fragments were then combined by overlap-extension PCR. The resulting fragment of *pmd17g* was digested with *Spe*I and *Bgl*II and cloned into the *Nhe*I/*Bam*HI-digested pYE22m

plasmid vector. The putative intron regions were determined by the comparison with *pmd17c* sequences.

***S. cerevisiae* transformation**

The constructs pYE22mPsulω3, pYE22mPmd17c, and pYE22mPmd17g were introduced into *S. cerevisiae* using the electroporation method and the Biorad Gene Pulser Xcell System according to the manufacturer's protocol (https://www.bio-rad.com/webroot/web/pdf/lsr/literature/4006217A.pdf).
Tryptophan-auxotrophic selection was used as the selection mechanism. The transformation was performed using SC sorbitol as a selection medium (0.17% Difco yeast nitrogen base w/o amino acids and ammonium sulfate, 0.5% $(NH_4)_2SO_4$, 2% glucose, 20 mg L^{-1} adenine, 30 mg L^{-1} tyrosine, 20 mg L^{-1} uracil, 10 mg L^{-1} methionine, 20 mg L^{-1} arginine, 20 mg L^{-1} histidine, 40 mg L^{-1} lysine, 50 mg L^{-1} threonine, 60 mg L^{-1} isoleucine, 60 mg L^{-1} leucine, 60 mg L^{-1} phenylalanine, 1 M sorbitol, and 2% agar).

Construction of plasmids for ω3 desaturase gene expression in *M. alpina*

The pBIG35ZhSSA2p plasmid vector previously constructed was used as a plasmid vector backbone (32). This backbone drives the expression of a target gene using the constitutive *SSA2* promoter and *sdhB* terminator. The original full-length *psulω3, pmd17c*, and *pmd17g* sequences were codon-optimized for expression in *M. alpina* based on the codon usage of *M. alpina* and synthesized by Life Technologies and designated *psulω3m, pmd17cm*, and *pmd17gm* to indicate the modified versions of these genes. These gene fragments contain *Spe*I and *Bam*HI restriction sites at the 5' and 3' ends, respectively. The synthesized gene fragments were digested with both the restriction enzymes *Spe*I and *Bam*HI, and then cloned into an *Spe*I/*Bam*HI-digested pBIG35ZhSSA2p plasmid vector. The resulting plasmid vectors containing *psulω3m, pmd17cm*, and *pmd17gm* were designated pBIGSSA2pPsulω3m, pBIGSSA2pPmd17cm, and pBIGSSA2pPmd17gm, respectively (**Figure 1.6**).

***M. alpina* transformation**

The plasmid vectors pBIGSSA2pPsulω3m, pBIGSSA2pPmd17cm, and pBIGSSA2pPmd17gm were introduced into *M. alpina* using the ATMT method described previously (30).

Analyses of fatty acid profiles and lipid content of *S. cerevisiae* and *M. alpina*

Cultivated cells were harvested (*S. cerevisiae* by centrifugation at 3000 × *g* for 10 min and other strains by filtration) and dried at 120 °C for 2 h. Fatty acids from the total cell lipids were analyzed as follows. First, 1 mg tricosanoic acid (C23:0) was added to each sample as an internal standard. The samples were then *trans*-methylated in 10% methanolic HCl at 55 °C for 3 h. The resulting fatty acid methyl esters (FAMEs) were extracted with 4 mL *n*-hexane, concentrated by a rotary evaporator, and then analyzed by gas chromatography (GC). Analysis of FAMEs was performed using a Shimadzu GC-2010 GC equipped with a 0.25 mm × 60 m TC-70 capillary column (GL sciences, Tokyo, Japan) and a flame ionization detector. The initial column temperature of 180 °C was held for 10 min, raised at 2 °C min^{-1} to 236 °C, then raised at 12 °C min^{-1} to 260 °C and held at 260 °C for 5 min. Fatty acids were identified by comparing their retention times with those of FAME standards (Sigma, USA) analyzed using the same GC conditions. Quantitation was carried out by comparing each peak area from the GC chromatogram with those from internal standards.

REFERENCES

1. P. Willatts, J. S. Forsyth, M. K. Dimodugno, S. Varma, M. Colvin, Effect of long-chain polyunsaturated fatty acids in infant formula on problem solving at 10 months of age. *Lancet* **352**, 688–691 (1998).
2. F. Shahidi, P. Ambigaipalan, Omega-3 polyunsaturated fatty acids and their health benefits. *Annu. Rev. Food Sci. Technol.* **9**, 345–381 (2018).
3. J. Dyerberg, H. O. Bang, O. Aagaard, α-linolenic acid and eicosapentaenoic acid. *Lancet* **315**, 199 (1980).
4. M. I. Gladyshev, N. N. Sushchik, O. N. Makhutova, Production of EPA and DHA in aquatic ecosystems and their transfer to the land. *Prostaglandins Other Lipid Mediat.* **107**, 117–126 (2013).
5. F. D. Gunstone, *Fatty Acid and Lipid Chemistry* (Springer, 1996) https:/doi.org/10.1007/978-1-4615-4131-8.
6. FAO, "The State of World Fisheries and Aquaculture 2018-Meeting the sustainable development goals" (2018).
7. B. Worm, *et al.*, Impacts of biodiversity loss on Ocean Ecosystem Services. *Science (80-.).* **314**, 787–790 (2006).
8. T. A. Walsh, *et al.*, Canola engineered with a microalgal polyketide synthase-like system produces oil enriched in docosahexaenoic acid. *Nat. Biotechnol.* **34**, 881–887 (2016).
9. M. A. Borowitzka, High-value products from microalgae-their development and commercialisation. *J. Appl. Phycol.* **25**, 743–756 (2013).
10. T. Okuda, A. Ando, E. Sakuradani, J. Ogawa, Isolation and characterization of a docosahexaenoic acid-phospholipids producing microorganism *Crypthecodinium* sp. D31. *J. Am. Oil Chem. Soc.* **90**, 1837–1844 (2013).
11. K. Watanabe, K. Yazawa, K. Kondo, A. Kawaguchi, Fatty acid synthesis of an eicosapentaenoic acid-producing bacterium: De novo synthesis, chain elongation, and desaturation systems. *J. Biochem.* **122**, 467–473 (1997).
12. Z. Cohen, The production potential of eicosapentaenoic and arachidonic acids by the red alga *porphyridium cruentum*. **67**, 916–920 (1990).
13. S. Otles, R. Pire, Fatty acid composition of *chlorella and spirulina* microalgae species.

J. AOAC Int. **84**, 1708–1714 (2001).

14. W. Yongmanitchai, O. P. Ward, Growth of and omega-3 fatty acid production by *Phaeodactylum tricornutum* under different culture conditions. *Appl. Environ. Microbiol.* **57**, 419–425 (1991).
15. C. K. Tan, M. R. Johns, Screening of diatoms for heterotrophic eicosapentaenoic acid production. *J. Appl. Phycol.* **8**, 59–64 (1996).
16. S. Shimizu, H. Kawashima, Y. Shinmen, K. Akimoto, H. Yamada, Production of eicosapentaenoic acid by *Mortierella* fungi. *J. Am. Oil Chem. Soc.* **65**, 1455–1459 (1988).
17. Z. Xue, *et al.*, Production of omega-3 eicosapentaenoic acid by metabolic engineering of *Yarrowia lipolytica*. *Nat. Biotechnol.* **31**, 734–740 (2013).
18. S. R. Gandhi, J. D. Weete, Production of the polyunsaturated fatty acids arachidonic acid and eicosapentaenoic acid by the fungus *Pythium ultimum*. *J. Gen. Microbiol.* **137**, 1825–1830 (1991).
19. J. L. Gellerman, H. Schlenk, Methyl-directed desaturation of arachidonic to eicosapentaenoic acid in the fungus, *Saprolegnia parasitica*. *Biochim. Biophys. Acta* **573**, 23–30 (1979).
20. D. J. O'Brien, M. J. Kurantz, R. Kwoczak, Production of eicosapentaenoic acid by the filamentous fungus *Pythium irregulare*. *Appl. Microbiol. Biotechnol.* **40**, 211–214 (1993).
21. E. E. Stinson, R. Kwoczak, M. J. Kurantz, Effect of cultural conditions on production of eicosapentaenoic acid by *Pythium irregulare*. *J. Ind. Microbiol.* **8**, 171–178 (1991).
22. B. Qi, *et al.*, Production of very long chain polyunsaturated omega-3 and omega-6 fatty acids in plants. *Nat. Biotechnol.* **22**, 739–745 (2004).
23. N. Ruiz-Lopez, R. P. Haslam, J. A. Napier, O. Sayanova, Successful high-level accumulation of fish oil omega-3 long-chain polyunsaturated fatty acids in a transgenic oilseed crop. *Plant J.* **77**, 198–208 (2014).
24. Y. Chen, D. Meesapyodsuk, X. Qiu, Transgenic production of omega-3 very long chain polyunsaturated fatty acids in plants: Accomplishment and challenge. *Biocatal. Agric. Biotechnol.* **3**, 38–43 (2014).
25. Y. Shinmen, S. Shimizu, K. Akimoto, H. Kawashima, H. Yamada, Production of arachidonic acid by *Mortierella* fungi - Selection of a potent producer and optimization

of culture conditions for large-scale production. *Appl. Microbiol. Biotechnol.* **31**, 11–16 (1989).

26. E. Sakuradani, A. Ando, J. Ogawa, S. Shimizu, Improved production of various polyunsaturated fatty acids through filamentous fungus *Mortierella alpina* breeding. *Appl. Microbiol. Biotechnol.* **84**, 1–10 (2009).
27. S. Takeno, *et al.*, Cloning and sequencing of the *ura3* and *ura5* genes, and isolation and characterization of uracil auxotrophs of the fungus *Mortierella alpina* 1S-4. *Biosci. Biotechnol. Biochem.* **68**, 277–285 (2004).
28. A. Ando, E. Sakuradani, K. Horinaka, J. Ogawa, S. Shimizu, Transformation of an oleaginous zygomycete *Mortierella alpina* 1S-4 with the carboxin resistance gene conferred by mutation of the iron-sulfur subunit of succinate dehydrogenase. *Curr. Genet.* **55**, 349–356 (2009).
29. S. Takeno, *et al.*, Establishment of an overall transformation system for an oil-producing filamentous fungus, *Mortierella alpina* 1S-4. *Appl. Microbiol. Biotechnol.* **65**, 419–425 (2004).
30. A. Ando, *et al.*, Establishment of Agrobacterium tumefaciens-mediated transformation of an oleaginous fungus, *Mortierella alpina* 1S-4, and its application for eicosapentaenoic acid producer breeding. *Appl. Environ. Microbiol.* **75**, 5529–5535 (2009).
31. T. Okuda, *et al.*, Characterization of galactose-dependent promoters from an oleaginous fungus *Mortierella alpina* 1S-4. *Curr. Genet.* **60**, 175–182 (2014).
32. T. Okuda, *et al.*, Selection and characterization of promoters based on genomic approach for the molecular breeding of oleaginous fungus *Mortierella alpina* 1S-4. *Curr. Genet.* **60**, 183–191 (2014).
33. H. Kikukawa, *et al.*, Gene targeting in the oil-producing fungus *Mortierella alpina* 1S-4 and construction of a strain producing a valuable polyunsaturated fatty acid. *Curr. Genet.* **61**, 579–589 (2015).
34. X. Tang, *et al.*, Characterization of an omega-3 desaturase from *Phytophthora parasitica* and application for eicosapentaenoic acid production in *Mortierella alpina*. *Front. Microbiol.* **9**, 1–9 (2018).
35. T. Okuda, *et al.*, Eicosapentaenoic acid (EPA) production by an oleaginous fungus *Mortierella alpina* expressing heterologous the Δ17-desaturase gene under ordinary

temperature. *Eur. J. Lipid Sci. Technol.* **117**, 1919–1927 (2015).

36. C. Ge, *et al.*, Application of a ω-3 desaturase with an arachidonic acid preference to eicosapentaenoic acid production in *Mortierella alpina*. *Front. Bioeng. Biotechnol.* **5**, 1–10 (2018).
37. D. Meesapyodsuk, *et al.*, Characterization of the regiochemistry and cryptoregiochemistry of a *Caenorhabditis elegans* fatty acid desaturase (*FAT-1*) expressed in *Saccharomyces cerevisiae*. *Biochemistry* **39**, 11948–11954 (2000).
38. T. Oura, S. Kajiwara, *Saccharomyces kluyveri FAD3* encodes an ω3 fatty acid desaturase. *Microbiology* **150**, 1983–1990 (2004).
39. E. Sakuradani, T. Abe, K. Iguchi, S. Shimizu, A novel fungal ω3-desaturase with wide substrate specificity from arachidonic acid-producing *Mortierella alpina* 1S-4. *Appl. Microbiol. Biotechnol.* **66**, 648–654 (2005).
40. S. L. Pereira, *et al.*, A novel ω3-fatty acid desaturase involved in the biosynthesis of eicosapentaenoic acid. *Biochem. J.* **378**, 665–671 (2004).
41. X. Zhang, M. Li, D. Wei, L. Xing, Identification and characterization of a novel yeast ω3-fatty acid desaturase acting on long-chain n-6 fatty acid substrates from *Pichia pastoris*. *Yeast* (2008) https:/doi.org/10.1002/yea.1546.
42. Z. Xue, *et al.*, Identification and characterization of new Δ-17 fatty acid desaturases. *Appl. Microbiol. Biotechnol.* **97**, 1973–1985 (2013).
43. C. Rong, *et al.*, Characterization and molecular docking of new Δ17 fatty acid desaturase genes from: *Rhizophagus irregularis* and *Octopus bimaculoides*. *RSC Adv.* **9**, 6871–6880 (2019).
44. P. Sperling, P. Ternes, T. K. Zank, E. Heinz, The evolution of desaturases. *Prostaglandins, Leukot. Essent. Fat. Acids* **68**, 73–95 (2003).
45. M. R. Jackson, T. Nilsson, P. A. Peterson, Identification of a consensus motif for retention of transmembrane proteins in the endoplasmic reticulum. *EMBO J.* **9**, 3153–3162 (1990).
46. K. H. D. Le, F. Lederer, On the presence of a heme-binding domain homologous to cytochrome b 5 in *Neurospora crassa* assimilatory nitrate reductase. *EMBO J.* **2**, 1909–1914 (1983).
47. K. Hashimoto, *et al.*, The repertoire of desaturases and elongases reveals fatty acid variations in 56 eukaryotic genomes. *J. Lipid Res.* **49**, 183–191 (2008).

48. H. Shi, *et al.*, Molecular mechanism of substrate specificity for delta 6 desaturase from *Mortierella alpina* and *Micromonas pusilla*. *J. Lipid Res.* **56**, 2309–2321 (2015).
49. C. Rong, *et al.*, Molecular mechanism of substrate preference for ω-3 fatty acid desaturase from *Mortierella alpina* by mutational analysis and molecular docking. *Appl. Microbiol. Biotechnol.* **102**, 9679–9689 (2018).
50. N. Kabeya, *et al.*, Genes for de novo biosynthesis of omega-3 polyunsaturated fatty acids are widespread in animals. *Sci. Adv.* **4**, 1–9 (2018).
51. E. Sakuradani, M. Kobayashi, S. Shimizu, δ9-Fatty acid desaturase from arachidonic acid-producing fungus. Unique gene sequence and its heterologous expression in a fungus, *Aspergillus*. *Eur. J. Biochem.* **260**, 208–216 (1999).
52. L. Dobson, I. Remenyi, G. E. Tusnady, CCTOP: A consensus constrained TOPology prediction web server. *Nucleic Acids Res.* **43**, W408–W412 (2015).
53. P. Cirpus, J. Bauer, T. Zank, E. Heinz, Method for producing unsaturated omega-3 fatty acids in transgenic organisms (2017).
54. The *C. elegans* Sequencing Consortium, Genome sequence of the nematode *C. elegans*: A platform for investigating biology. *Science (80-.).* **282**, 2012–2018 (1998).
55. L. Wang, *et al.*, Genome Characterization of the Oleaginous Fungus *Mortierella alpina*. *PLoS One* **6**, e28319 (2011).
56. H. G. Damude, *et al.*, Identification of bifunctional Δ12/ω3 fatty acid desaturases for improving the ratio of ω3 to ω6 fatty acids in microbes and plants. *Proc. Natl. Acad. Sci. U. S. A.* (2006) https:/doi.org/10.1073/pnas.0511079103.
57. R. C. Edgar, MUSCLE: Multiple sequence alignment with high accuracy and high throughput. *Nucleic Acids Res.* **32**, 1792–1797 (2004).
58. S. Kumar, G. Stecher, M. Li, C. Knyaz, K. Tamura, MEGA X: Molecular Evolutionary Genetics Analysis across Computing Platforms. *Mol. Biol. Evol.* **35**, 1547–1549 (2018).
59. D. T. Jones, W. R. Taylor, J. M. Thornton, The rapid generation of mutation data matrices from protein sequences. *Bioinformatics* **8**, 275–282 (1992).

CHAPTER 2

Establishment of a platform organism *Basidiobolus meristosporus* for free fatty acid derivative production

SECTION 1

Free fatty acid production by the oleaginous fungus *Basidiobolus meristosporus*

ABSTRACT

Free fatty acid (FFA) derivatives fermented from biomass are potential alternative sources for various functional lipids and industrial oleochemicals, but no reported organisms accumulate high levels of FFA without extensive metabolic engineering. In this study, a filamentous fungus *Basidiobolus meristosporus* NBRC 108890 with a metabolic environment intrinsically tailored for FFA production is described. Results show that FFAs are produced to high levels from glucose, constituting 87.2% of total fatty acids, and reaching an FFA titer of 10.0 g L^{-1}, productivity of 61.7 mg L^{-1} h^{-1} and yield of 0.05 g FFAs g^{-1} glucose (~17% of the theoretical maximum) after 162 h of fed-batch cultivation at flask scale. This organism is a potential platform strain for the bioproduction of FFA-derived oleochemicals.

INTRODUCTION

Current liquid fuels and oleochemicals are mainly purified from fossil resources, which is unsustainable and unrenewable. The reliance on fossil fuels is particularly problematic as it is the main cause of climate change (1, 2). There has thus been interest in producing functional lipids and industrial oleochemicals from renewable and photosynthesis-derived sugars by engineered microorganisms (3). Bioproduction through the free fatty acid (FFA) pathway is of particular interest as FFAs can be converted via one or two-step enzyme-catalyzed reactions to various fuels, fragrances, emollients, plasticizers, thickeners, detergents, and preservatives (3, 4).

However, microorganisms currently used for FFA production suffer from low native FFA titers (5–7) and tight fatty acid regulation at the transcriptional and product feedback levels (8–11). FFA titers of wild type platform microorganisms are ~0.02 mg L^{-1} in *Escherichia coli* BL21 (5), ~100 mg L^{-1} in *Saccharomyces cerevisiae* (6), and ~30.2 mg L^{-1} in *Yarrowia lipolytica* (7), which are industrially irrelevant. FFA production has thus necessitated extensive engineering of their central carbon metabolic pathways (12–14). A microorganism with endogenous FFA accumulation would greatly simplify subsequent metabolic engineering and could potentially facilitate more cost-effective FFA production, but to date such an organism has not been reported to date. While the bacterium GK12 reportedly accumulates FFAs (15), solvent stress conditions that may impact growth were needed, key production metrics such as titer and yield were not evaluated, and the organism was unavailable in microbial culture repositories.

This study thus aimed to identify a microorganism that endogenously accumulates FFAs. Stocked fungi that were known to accumulate lipids were screened for FFA production, leading to a focus on *Basidiobolus* spp. as it contained a member known to produce FFAs. After further research on several *Basidiobolus* strains, an oleaginous fungus with significant intrinsic FFA production, *Basidiobolus meristosporus*, was discovered. Its potential for application as an FFA-derivative production platform was then evaluated.

RESULTS

Screening for oleaginous fungi with high level FFA production

Screening of stocked fungal strains of the divisions Entomophthoromycota and Mucoromycota showed that the filamentous fungus *Basidiobolus* sp. accumulated FFAs. Nine *Basidiobolus* strains were thus obtained from NBRC for further selection (Refer to "Materials and Methods"). Intracellular lipids of the nine strains were subjected to trimethylsilyldiazomethane methylation of FFAs and subsequent gas chromatography (GC) to quantify FFA production. As a result, *B. ranarum* NBRC 106086 and *B. meristosporus* NBRC 108890 showed outstanding growth and FFA production. After 5 d cultivation, the dry cell weights (DCW) of *B. ranarum* NBRC 106086 and *B. meristosporus* NBRC 108890 reached 11.28 g L^{-1} and 12.73 g L^{-1} respectively, while the other strains were less than 8 g L^{-1} (**Figure 2.1**). FFA production of *B. ranarum* NBRC 106086 and *B. meristosporus* NBRC 108890 reached 2.02 g L^{-1} and 1.32 g L^{-1} respectively, while the other strains produced less than 0.7 g L^{-1}. Although *B. ranarum* NBRC 106086 grew to the highest cell density and produced the most FFAs, *B. meristosporus* NBRC 108890 was selected for further analysis due to the pathogenic nature of *B. ranarum* (16–20).

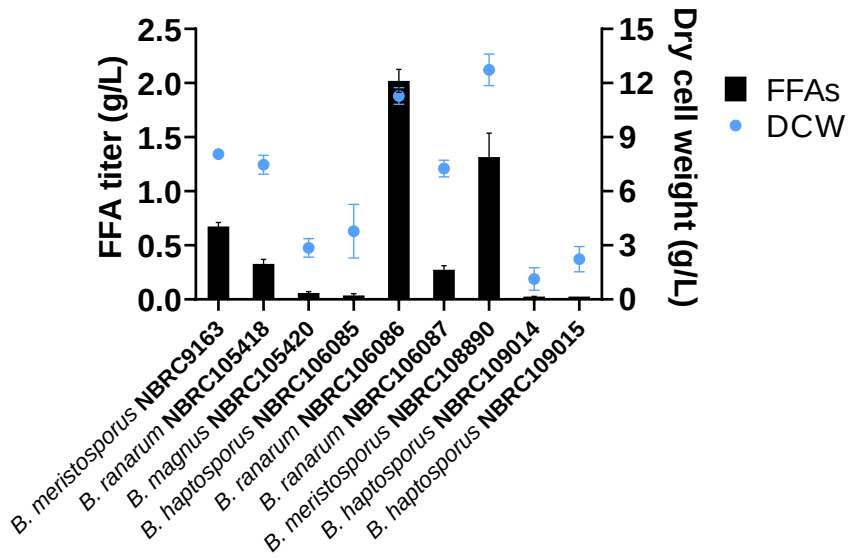

Figure 2.1. Growth and free fatty acid (FFA) production of NBRC *Basidiobolus* spp. (n=3, error bars represent standard deviation of the mean).

B. meristosporus NBRC 108890 showed white, flat, and smooth physiology when grown on potato dextrose agar (PDA) (**Figure 2.2a**) and could ballistically project ballistospores (**Figure 2.2b**) from its mycelial apices. The ejected ballistospores showed mycelial beaks characteristic of *Basidiobolus* species and germinated to form satellite colonies after three days growth on PDA.

(a)

(b)

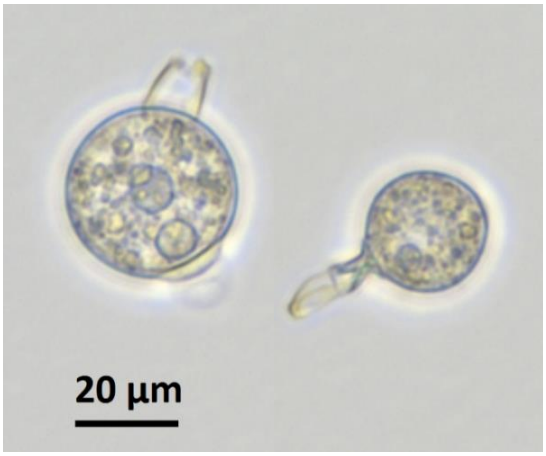

Figure 2.2. (a) Mycelial growth of *B. meristosporus* NBRC 108890 showing satellite colonies formed by germinated ballistic spores. (b) Discharged ballistospores with mycelial beaks.

Characterization of *B. meristosporus* FFA production

To characterize FFA production in *B. meristosporus* NBRC 108890, a fed-batch fermentation at 300 mL flask scale was conducted (**Figure 2.3**). Residual glucose measurements indicated that the glucose consumption rate was highest during early to mid fermentation (approximately 50 to 180 h). Cell growth similarly increased throughout early to late fermentation, reaching a maximum DCW of 42.2 g L^{-1} after 312 h cultivation. Derivatization of cellular FFAs and subsequent GC analysis showed that the FFA titer increased until 162 h, then decreased from 162 to 312 h. After 162 h, *B. meristosporus* produced an FFA titer of 10.0 g L^{-1}, a productivity of 61.7 mg L^{-1} h^{-1}, and a yield of 0.05 g FFA g^{-1} glucose (~17% of the theoretical maximum). FFAs comprised 5.4%, 27.5%, and 9.0% of DCW at 44, 162, and 312 h respectively.

The FFA species produced comprised of C12 to C20 species with varying degrees of saturation (**Figures 2.4a and b**). Major species at 162 h were 14:0 (0.21 g L^{-1}, 2.1% of total), 16:0 (2.48 g L^{-1}, 24.7%), 16:1 (0.57 g L^{-1}, 5.7%), 18:0 (0.80 g L^{-1}, 7.9%), 18:1 (2.98 g L^{-1}, 29.7%), 18:2 (1.25 g L^{-1}, 12.5%), and 18:3 (0.13 g L^{-1}, 1.3%), while the other species mainly consisted of 12:0, 14:1, 16:2, and 20:0. This FFA composition closely resembled the total fatty acid (TFA) composition (Data not shown).

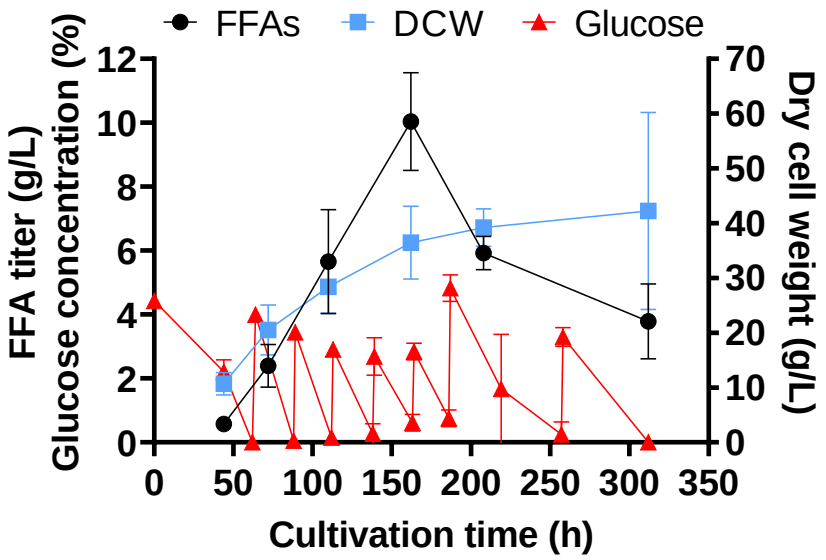

Figure 2.3. FFA production, cell growth, and glucose uptake of *B. meristosporus* during fed-batch fermentation at 300 mL flask scale. (n=3, error bars represent standard deviation of the mean).

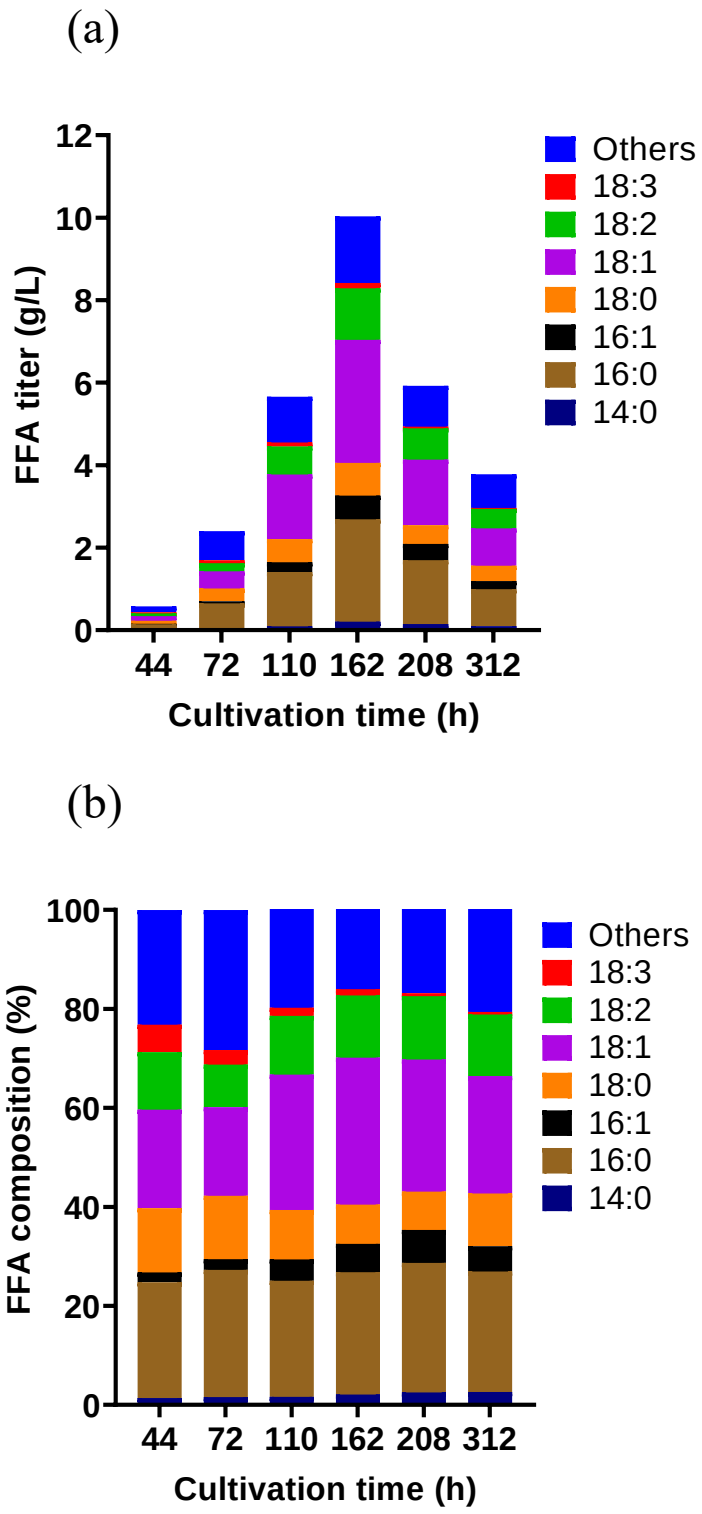

Figure 2.4. (a) FFA production and (b) composition of *B. meristosporus* during fed-batch fermentation at 300 mL flask scale. 14:0, myristic acid; 16:0, palmitic acid; 16:1, palmitoleic acid; 18:0, stearic acid; 18:1, oleic acid; 18:2, linoleic acid; 18:3, γ-linolenic acid. (n=3).

Lipid class analysis of *B. meristosporus*

Cultivated mycelium representative of early, mid, and late stage fermentation (72, 162, and 312 h) were then used for lipid class analysis. The extracted lipids were first separated by thin layer chromatography (TLC), visualized after primuline dyeing and compared to various standards. Six main fractions were present for all samples, corresponding to sterol esters, triacylglycerols, FFAs, diacylglycerols or sterols, and polar lipids (**Figure 2.5a**).

The lipid class ratio was then calculated by scraping, extraction, and GC analysis of the respective spots corresponding to the different lipid classes. As a result, FFAs comprised 78.1%, 87.2%, and 57.3% of TFAs at 72 h, 162 h, and 312 h respectively (**Figure 2.5b**). At 162 h, the other lipid classes consisted of sterol esters (1.7%), triacylglycerols (3.3%), diacylglycerols or sterols (6.9%), and other polar lipids (0.8%).

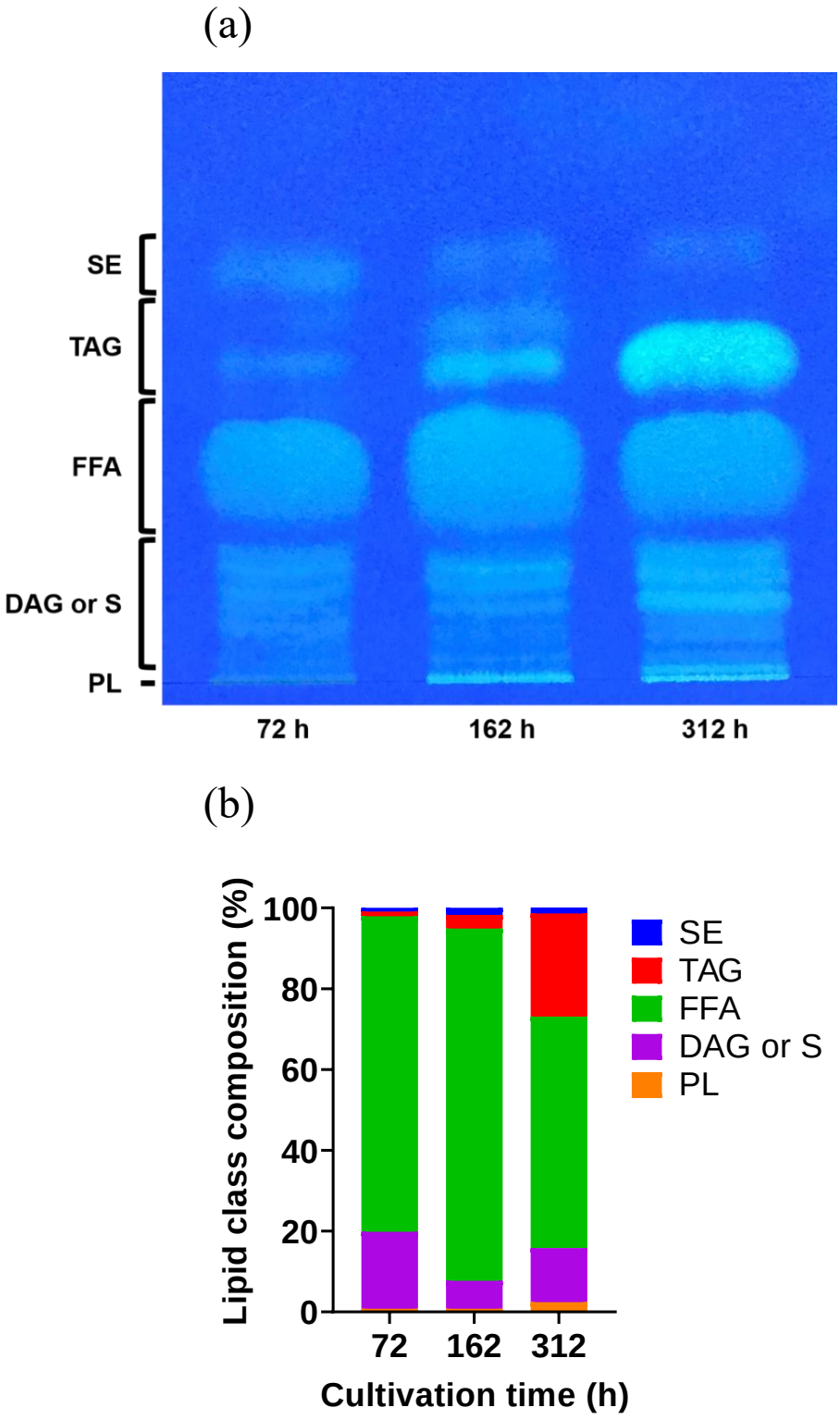

Figure 2.5. (a) Thin layer chromatography of lipids extracted from the mycelium (b) Lipid class composition of lipids extracted from the mycelium. SE, sterol esters; TAG, triacylglycerols; FFA, free fatty acids; DAG, diacylglycerols; S, Sterols; PL. polar lipids. (n=3)

DISCUSSION

Microbial production of FFA derivatives to date has utilized platform strains that produce low levels of FFAs, as no microorganisms reported to date produce large amounts of FFAs. In this study, an oleaginous fungus *B. meristosporus* NBRC 108890 with the ability to produce significant levels of FFAs was discovered.

During initial screening of oleaginous fungi with FFA producing ability, two *Basidiobolus* strains with outstanding FFA production ability were discovered, *B. ranarum* and *B. meristosporus* (**Figure 2.1**). *B. ranarum* is a human pathogen that causes gastrointestinal and subcutaneous zygomycosis (16–20), which is detrimental for industrial application. While *B. meristosporus* was previously suggested to be a human pathogen due to taxonomic confusion, it is now known that *B. ranarum* is the only *Basidiobolus* species causing rare fungal mycosis in humans and lower animals (16). *B. meristosporus* was therefore selected for further evaluation.

B. meristosporus is sufficiently phenotypically stable and tractable for use as a chassis organism. The traits of FFA production and sporogenesis were not noticeably impacted after several spore-mycelium life cycles, suggesting long-term stability. Harvesting the mycelium by vacuum filtration was fast and simple, although lipid extraction requires mechanical disruption by metal corn or glass beads to sufficiently lyze the cell wall and release FFAs.

B. meristosporus was also able to utilize commonly used industrial carbon and nitrogen sources and showed a robust tolerance to harsh cultivation conditions. During optimization of cultivation conditions for FFA production (Data not shown), *B. meristosporus* could utilize as carbon sources glycerol and the lignocellulose-derived hexoses glucose, mannose, and galactose. It also metabolized low-cost complex nitrogen sources such as corn steep soluble, yeast extract, polypeptone, soybean meal, and rice bran. Growth was observed at a wide pH range of pH 5–9 and a wide temperature range of 20-37 °C.

As lipid accumulation exceeded 20% of biomass (FFA production reached 27.5% DCW at 162 h), *B. meristosporus* is classified as an oleaginous fungus (21). However, while known oleaginous microorganisms accumulate triacylglycerols (TAGs) (21), *B. meristosporus* consistently accumulated the majority of lipids as FFAs (**Figure 2.5b**). This represents the first report of a microorganism with cellular lipids mainly consisting of FFAs. From 72 to 162 h, FFA/TFA increased, while from 162 h to 312 h FFA/TFA dropped and TAG/TFA increased.

This suggests that FFAs are accumulated during early to mid fermentation and incorporated into TAGs during mid to late fermentation, possibly due to changes in acyltransferase activity during growth.

During fed-batch fermentation, *B. meristosporus* produced significant amounts of FFAs. Compared to the FFA titers of current FFA derivative production platforms (Wild type *E. coli*, *S. cerevisiae*, and *Y. lipolytica*) (5–7), the FFA titer produced by *B. meristosporus* (10.0 g L^{-1} at 162 h) (**Figure 2.3**) represented ~500000-fold, ~100-fold and ~330-fold increases, respectively. Despite only having undergone a brief optimization, the production metrics produced by *B. meristosporus* were already comparable to those of extensively engineered microorganisms at bioreactor scale (12–14). It is thus expected that metabolic engineering and optimizing other parameters at bioreactor scale such as dissolved oxygen level, glucose consumption rate, pH, and temperature should further increase these production metrics. In addition, the produced FFAs mainly comprised of C16 and C18 FFAs (**Figure 2.4a**), which are substrates for biodiesel range hydrocarbons and various industrial and high-value chemicals (3, 4).

B. meristosporus evidently contains a metabolic environment tailored for FFA accumulation, and future work should focus on elucidating its biochemical basis. Genome sequencing should be a priority as it would provide a platform for the prediction of metabolism and gene function analysis. The high FFA content may be a result of novel mitochondrial thioesterases acting on C18 acyl-CoA during early/mid fermentation (0-162 h). During early/mid fermentation, lipids in the cell mostly consist of FFAs (**Figure 2.5b**); since fatty acid biosynthesis utilizes acyl-ACP for C16 FA synthesis and acyl-CoA for further elongation and mostly C18 FFA species are produced during this period (**Figure 2.4b**), it is possible that novel thioesterases may be catalyzing efficient acyl-CoA to FFA conversion during early/mid stage fermentation. An alternative hypothesis is that enzymes of the FFA biosynthetic pathway are unusually active, causing accumulation of FFAs due to a bottleneck in FFA degradation. Fatty acid transport may also be a factor, as peroxisomal β-oxidation may be inhibited by low rates of FFA/FFA-CoA transport from the cytosol to peroxisome oxidation. Regardless, the establishment of genetic tools such as gene expression elements, selection markers and transformation techniques would aid in the elucidation of fatty acid metabolism and future metabolic engineering studies. FFA-derived fuels and oleochemicals could then be heterologously produced from the endogenous FFA pool.

MATERIALS AND METHODS

Strain and culture conditions

For initial strain screening, nine strains (*Basidiobolus meristosporus* (NBRC 9163), *Basidiobolus ranarum* (NBRC 105418), *Basidiobolus magnus* (NBRC 105420), *Basidiobolus haptosporus* (NBRC 106085), *Basidiobolus ranarum* (NBRC 106086), *Basidiobolus ranarum* (NBRC 106087), *Basidiobolus meristosporus* (NBRC 108890), *Basidiobolus haptosporus* (NBRC 109014, *Basidiobolus haptosporus* (NBRC 109015)) were purchased from NBRC and maintained on PDA (3.9% potato dextrose agar) slants. They were transferred directly from slants to 12 mL GP44 medium (4% (w/v) glucose and 4% (w/v) hipolypepton S (Nihon Pharmaceutical, Japan), initial pH adjusted to 7 and autoclaved) in 60 mL test tubes and incubated at 28 °C with shaking at 250 strokes min^{-1} for five days. Organisms with level 2 biosafety statuses were handled in accordance with the National Institutes of Health established criteria.

For fed-batch fermentation of *B. meristosporus* NBRC 108890, mycelium from PDA slants were transferred to 90 mm PDA plates and statically incubated at 28 °C for two days. Three discs (3 mm diameter) were excised from the outer perimeter and used as inoculum for each flask. Fed-batch fermentations were carried out using 15 mL of GP44 medium in 300 mL baffled Erlenmeyer flasks (Sibata, Japan) with silicone caps (Model C-40, AS ONE, Japan) at 28 °C, and shaking at 100 rpm (orbit diameter 70 mm). Glucose (937.5 µL, 64%) and hipolypepton S (1875 µL, 32%) were added to the medium as glucose dropped below 1% (62, 88, 112, 138, and 162 h). Glucose (1875 µL, 64%) and hipolypepton S (3750 µL, 32%) were added to the medium at 187 and 257 h.

Glucose measurement

Residual glucose levels were quantified with the WAKO glucose II kit (Wako, Japan).

Dry cell weight measurements, lipid extraction and TFA/FFA analysis by gas chromatography

Time point samples for lipid quantification were stored at -20 °C for future analysis. Mycelium was harvested by vacuum filtration and dried for 36 h using a freeze dryer (EYELA, Japan). DCW was then measured by a mechanical scale.

For lipid extraction, approximately 50 mg of dried cells were used and the ratio of used cells/total cells was recorded. The cells were transferred to a bead-beating tube (WATSON, Japan) with 1 mL of added water and homogenized at 5000 revolutions min^{-1} for 2 min. 0.5 mg tricosanoic acid (23:0) was added to each sample as an internal standard, and the lipids were extracted by the Bligh-Dyer method as previously stated (22).

For FFA analysis, approximately 1 mg lipids were transferred to test tubes and analyzed by a modified version of a method utilizing trimethylsilyldiazomethane described previously (22). The lipids were dissolved in 5 mL methanol/benzene (2:3) and methylated with 150 µL 1% trimethylsilyldiazomethane in hexane at 28 °C for 30 min. The resulting fatty acid methyl esters were analyzed by GC as previously stated. FFA concentration was calculated by the corresponding fatty acid/internal standard peak area. For calculation of FFA titer, the sum of the initial medium volume and the fed solution volume was used.

Lipid class analysis by thin layer chromatography

For semi-quantitative TLC analysis, extracted lipids from 150 mg of dried cells were spotted on a 20 × 20 cm aluminum backed TLC silica gel plate (1.05554.0001, Merck, Germany), and developed using hexane:diethyl ether:acetic acid (80:30:1). The plate was dyed by spraying with 0.01% primuline in 80% acetone then visualized under UV light. Spots corresponding to different lipid classes were identified using various standards, then scraped and deposited to separate test tubes. 4 mL ethyl acetate containing 0.2 mg tricosanoic acid (23:0) internal standard was inserted, and the mixture was vortexed for 30 s, then centrifuged at 3000 × *g* for 10 min. The supernatant was transferred to a new test tube and evaporated under reduced pressure in a rotary evaporator. The lipids were then trans-methylated in 10% methanolic HCl at 55 °C for 4 h. The resulting fatty acid methyl esters (FAMEs) were extracted using 4 mL hexane, concentrated using a rotary evaporator, then analyzed by GC as previously stated (22). The lipid class ratios were calculated by the total fatty acid/internal standard peak areas.

REFERENCES

1. United Nations Environment Programme, “Emissions Gap Report 2019” (2019).
2. IPCC, *Climate change 2014: synthesis report* (2014).
3. J. D. Keasling, Manufacturing molecules through metabolic engineering. *Science (80-.).* **330**, 1355–1358 (2010).
4. A. Q. Yu, N. K. Pratomo Juwono, S. S. J. Leong, M. W. Chang, Production of fatty acid-derived valuable chemicals in synthetic microbes. *Front. Bioeng. Biotechnol.* **2**, 1–12 (2014).
5. X. Lu, H. Vora, C. Khosla, Overproduction of free fatty acids in *E. coli*: Implications for biodiesel production. *Metab. Eng.* **10**, 333–339 (2008).
6. L. Chen, J. Zhang, J. Lee, W. N. Chen, Enhancement of free fatty acid production in *Saccharomyces cerevisiae* by control of fatty acyl-CoA metabolism. *Appl. Microbiol. Biotechnol.* **98**, 6739–6750 (2014).
7. E. Y. Yuzbasheva, *et al.*, A metabolic engineering strategy for producing free fatty acids by the *Yarrowia lipolytica* yeast based on impairment of glycerol metabolism. *Biotechnol. Bioeng.* **115**, 433–443 (2018).
8. H. J. Janßen, A. Steinbüchel, Fatty acid synthesis in *Escherichia coli* and its applications towards the production of fatty acid based biofuels. *Biotechnol. Biofuels* **7**, 1–26 (2014).
9. O. Tehlivets, K. Scheuringer, S. D. Kohlwein, Fatty acid synthesis and elongation in yeast. *Biochim. Biophys. Acta - Mol. Cell Biol. Lipids* **1771**, 255–270 (2007).
10. M. Dourou, D. Aggeli, S. Papanikolaou, G. Aggelis, Critical steps in carbon metabolism affecting lipid accumulation and their regulation in oleaginous microorganisms. *Appl. Microbiol. Biotechnol.* **102**, 2509–2523 (2018).
11. D. Xie, Integrating cellular and bioprocess engineering in the non-conventional yeast *Yarrowia lipolytica* for biodiesel production: A review. *Front. Bioeng. Biotechnol.* **5** (2017).
12. Y. Xiao, C. H. Bowen, D. Liu, F. Zhang, Exploiting nongenetic cell-to-cell variation for enhanced biosynthesis. *Nat. Chem. Biol.* **12**, 339–344 (2016).
13. T. Yu, *et al.*, Reprogramming Yeast Metabolism from Alcoholic Fermentation to Lipogenesis. *Cell* **174**, 1549-1558.e14 (2018).

14. R. Ledesma-Amaro, R. Dulermo, X. Niehus, J. M. Nicaud, Combining metabolic engineering and process optimization to improve production and secretion of fatty acids. *Metab. Eng.* **38**, 38–46 (2016).
15. T. Katayama, *et al.*, An oleaginous bacterium that intrinsically accumulates long-chain free fatty acids in its cytoplasm. *Appl. Environ. Microbiol.* **80**, 1126–1131 (2014).
16. R. Vilela, L. Mendoza, Human pathogenic entomophthorales. *Clin. Microbiol. Rev.* **31**, 1–40 (2018).
17. M. H. F. El-Shabrawi, N. M. Kamal, Gastrointestinal basidiobolomycosis in children: An overlooked emerging infection? *J. Med. Microbiol.* **60**, 871–880 (2011).
18. L. Mendoza, *et al.*, Human fungal pathogens of Mucorales and Entomophthorales. *Cold Spring Harb. Perspect. Med.* **5**, 1–34 (2015).
19. H. C. Gugnani, A review of zygomycosis due to *Basidiobolus ranarum*. *Eur. J. Epidemiol.* (1999) https:/doi.org/10.1023/A:1007656818038.
20. M. Anand, S. D. Deshmukh, D. P. Pande, S. Naik, D. P. Ghadage, Subcutaneous zygomycosis due to *basidiobolus ranarum*: A case report from Maharastra, India. *J. Trop. Med.* **2010**, 10–12 (2010).
21. C. Ratledge, J. P. Wynn, The biochemistry and molecular biology of lipid accumulation in oleaginous microorganisms. *Adv. Appl. Microbiol.* **51**, 1–52 (2002).
22. S. Kishino, *et al.*, Polyunsaturated fatty acid saturation by gut lactic acid bacteria affecting host lipid composition. *Proc. Natl. Acad. Sci. U. S. A.* **110**, 17808–17813 (2013).

SECTION 2

Development of a host-vector system for free fatty acid derivative production by the oleaginous fungus *Basidiobolus meristosporus*

ABSTRACT

The oleaginous fungus *Basidiobolus meristosporus* NBRC 108890 accumulates a significant amount of free fatty acids (FFA) and is a potential host for FFA derivative production. In this study, a transformation system utilizing a plasmid vector containing a carboxin resistance gene as a selection marker and a β-glucuronidase (GUS) gene as an expression reporter is described. After transformation into the ballistospores by biolistic bombardment, the resulting transformants could be recovered on carboxin selective plates after 72 hours and showed stable GUS activity. Transformation efficiency reached approximately 237 transformants/10^6 ballistospores. Using this transformation system, the fatty acid hydratase gene *FA-HY1* was expressed, which catalyzes the hydration of linoleic acid FFA to 13-hydroxy-*cis*-9-octadecenoic acid FFA. A resulting transformant produced 13-hydroxy-*cis*-9-octadecenoic acid from glucose to a titer of 311 mg L^{-1} after 186 h of incubation. This transformation system should facilitate the sustainable production of industrially relevant FFA derivatives.

INTRODUCTION

Oleochemicals are currently obtained mainly from the purification of unsustainable sources such as fossil, plant, and animal resources. The reliance on fossil fuels is particularly problematic as it is the main cause of climate change (1, 2). There has thus been interest in their production from renewable, photosynthesis-derived sugars by engineered microorganisms (3). Bioproduction through the free fatty acid (FFA) pathway is of particular interest as FFAs can be quantified more simply than acyl-CoA and acyl-ACP (4), and FFAs can be converted via one or two-step enzyme-catalyzed reactions to various FFA-derivatives such as fuels, fragrances, emollients, plasticizers, thickeners, detergents, preservatives, and high-value chemicals (3, 5). For example, hydroxy fatty acids are widely used as industrial chemicals and are suggested to be gut metabolites of physiological significance (6–8), and can be produced by fatty acid hydratase-catalyzed conversion of FFAs (9). While hydroxy fatty acid production by enzymatic reaction and cell biotransformation has been widely reported (10–12), reports of hydroxy fatty acid production from glucose has been limited to date. Moreover, those studies have exclusively utilized the industrial workhorses *E. coli* and *S. cerevisiae* (13–18).

To date, the well-studied model organisms *Escherichia coli*, *Saccharomyces cerevisiae*, and *Yarrowia lipolytica* have been used to produce FFA-derived oleochemicals, but these organisms suffer from limited endogenous production of FFA due to tight fatty acid regulation at the transcriptional and product feedback levels (19–24). The production of FFAs in these organisms have thus required extensive reengineering of their central carbon metabolisms (25–27). *Basidiobolus meristosporus* has been suggested as an alternative host to produce FFA-derivatives as it endogenously accumulates FFAs, grows rapidly (Refer to chapter 1), and tolerates levels of FFAs that are cytotoxic to many microorganisms (28). The wild type (WT) inherently accumulates FFAs to up to 87.2% of total fatty acids and an FFA titer of 10 g L^{-1} (Refer to chapter 2.1), does not secrete any known toxins and can grow rapidly to densities of ~50 g L^{-1} dry cell weight. *B. meristosporus* is thus thought to have high potential as a platform strain for FFA derivative production. However, metabolic engineering has not been possible to date due to the lack of basic genetic tools such as gene expression control elements, selection markers, viable plasmid vector backbones, and transformation techniques.

This study thus aimed to develop a rapid transformation system for *B. meristosporus* to enable the expression of foreign DNA and the subsequent selection of transformed colonies. In this study, methods for heterologous gene expression and transformant recovery using carboxin resistance as a dominant selection mechanism were developed. Using this developed transformation system, the feasibility of *B. meristosporus* to produce FFA derivatives was analyzed via expression of a fatty acid hydratase catalyzing the conversion of linoleic acid FFA to 13-hydroxy-*cis*-9-octadecenoic acid FFA.

RESULTS

Preparation of target cells

Single-celled spores are desirable as target cells as they enable quantification of transformation efficiency and ease of colony isolation. Since *Basidiobolus ranarum* readily discharges large amounts of ballistospores at high velocity (29) under certain conditions, it was hypothesized that *B. meristosporus* possessed a similar mechanism. After incubation on PDA medium for two or more days, large amounts of satellite colonies that were formed by germinated ballistospores were observed around the perimeter of the mycelial mass (Refer to chapter 2.1). By inverted incubation, this spore discharge mechanism was manipulated to deposit ballistospores on the lid of the dish, and germination was successfully inhibited. The spores could then be collected by gentle dislodging using a plastic spreader in the presence of 0.05% Tween 80. Using this method, approximately 2×10^5 ballistospores/150 mm plate were collected after seven days of incubation.

Antibiotic and fungicide susceptibility

Many transformation systems use an antibiotic and a gene conferring antibiotic resistance for the selection of transformants. In the filamentous fungus *Mortierella alpina*, 20 mg mL^{-1} zeocin or 100µg mL^{-1} carboxin (5,6-dihydro-2-methyl-1,4-oxathiine-3-carboxanilide) have been employed as selection mechanisms (30). The susceptibility of *B. meristosporus* to these two compounds and hygromycin B, which is also commonly used as a selection marker in filamentous fungi (31), were thus evaluated. At the low concentrations of antibiotics and fungicides tested (10-300 µg mL^{-1}) (**Table 2.1**), *B. meristosporus* showed no susceptibility to zeocin and hygromycin B. On the other hand, carboxin significantly inhibited mycelial growth after five days incubation with a minimum inhibitory concentration of 100 µg mL^{-1} and marginal background growth. Carboxin was thus chosen as a potential selection mechanism.

Table 2.1. *B. meristosporus* growth after 5 days cultivation on PDA supplemented with various concentrations of antibiotic or fungicide.

		Concentration (µg mL^{-1})					
		10	50	100	150	200	300
Antibiotic/fungicide	Hygromycin B	+	+	+	+	+	+
	Zeocin	+	+	+	+	+	+
	Carboxin	+	+	-	-	-	-

+, visible growth; -, no visible growth

Cloning of plasmid vector components

Carboxin inhibits the growth of susceptible fungi by blocking succinate dehydrogenase-catalyzed oxidation of succinate to fumarate in the mitochondria (32). In several fungi including the filamentous fungus *M. alpina*, substitution of a histidine residue in the third conserved cysteine-rich region of the succinate dehydrogenase iron-sulfur protein *sdhB* (**Figure 2.7**, third red box) confers resistance to carboxin (30, 33, 34). This mechanism was manipulated in *M. alpina* for use as a dominant selection marker (30). As *sdhB* and the critical histidine residue is conserved in many fungi, it was hypothesized that a similar approach was feasible as a dominant selection mechanism for *B. meristosporus*.

A 1151 bp fragment that showed 98% homology with the hypothetical *sdhB* region in *B. meristosporus* CBS 931.73 was amplified by touchdown PCR using *B. meristosporus* NBRC 108890 cDNA as a template. Observation of possible open reading frames led to the identification of a putative *sdhB* gene 867 bp in length (**Figure 2.6a**). Comparison of this amino acid sequence to *M. alpina* SDHB revealed a high degree of similarity; the three cysteine-rich clusters required to adhere to the iron-sulfur center were conserved to a high degree (**Figure 2.7**, red boxes), and the histidine residue in the third cluster was also present. This histidine residue was substituted with leucine via a single point mutation of A to T (**Figure 2.6a**, grey) to produce a mutant version of the *sdhB* gene (*CarR*).

Additionally, from *B. meristosporus* NBRC 108890 genomic DNA, 786 bp and 319 bp sequences containing the putative *sdhB* promoter and terminator sequences (**Figure 2.6b and c**) were amplified using oligonucleotide primers based on the *B. meristosporus* CBS 931.73 genome and the *B. meristosporus* NBRC 108890 *sdhB* gene, respectively (**Table 2.2**). Finally, a *β*-glucuronidase expression marker gene *GUSm* that was codon optimized for *M. alpina* (35) was cloned, as *M. alpina* and *B. meristosporus* CBS 931.73 showed similar codon bias based on codon usage comparison of several genes.

(a)

ATGTCAGCCTCACTTTTGACTATCGCTTCCAGAGCTTCCAGACCGCTCACTAGACA
AGCTGCACCAATGTTCACTAGTGTCGGAGTGAGAGGCTTCCAGTCTGGTCCAGTCC
CTCAAGCAAGTGAGGAAGCCCCCGCCCCTACCAGTAAAGCACCACTGTACAAAAC
TTTTTCTATCTATCGCTGGAACCCTGACGAGCCTACCGAGAAGCCCAAATTACAAG
ACTACACCATCGATGTAAACACCTGTGGCCCTATGGTCCTTGACGCTCTATTAAAAA
TCAAGAACGAGATTGACCCTACTTTAACTTTCCGTCGTTCCTGCCGTGAAGGTATTT
GCGGTTCATGTGCTATGAACATATATGGTGGTAACACCCTTGCTTGTATCTGTAAGAT
CGAGCGCGAAGAAAAAGCCGCCGTCAAGATTTACCCACTGCCTCATATGTATGTCG
TCAAAGATTTGGTCCCCGATTTGAACAACTTCTATAAGCAATACAAGAGCATCGAG
CCTTACCTCAAGCAGAAGAGTCCACTGAAGGAGGGAGCACGTGAGAACCTTCAG
AGCATTGAGGATCGTAAGAAGCTGGATGGCCTATACGAGTGCATTCTTTGTGCATGC
TGTTCTACCTCTTGCCCCTCTTACTGGTGGAATCAAGATGAATACCTTGGCCCCGCA
GTTTTGATGCAAGCCTACCGCTGGATGATCGATTCCAGAGATGAATATGGATCGGAA
CGTCGTGAAAAACTACAAAACCCCTTCAGTTTATACCGCTGCCACACAATCATGAA
CTGTGCTAGAACATGTCCTAAAGGCCTCAACCCTGGTAAAGCCATTGCCGAAATTA
AGAAGTTGATGGCAGCCGAATAA

(b)

ATTCTCGGTTAGGAAGTTGACTTGACAGAAAATAAAAATCTGCTTGACACCAAAGT
CCAGCAATACGAAATGACCCGAGAAAGTTGTCTCATACTCGGACAAATTGGGGCGT
GATGATTGGCCATCAGAGTCAAGATGCCGAGCTCGTGCTACGTGATGACTGACGTG
GGAAACGAACATCACTATGTGGAAGAGTTCGGTACGGTATTGAGACACTGCACTCC
CTATACAATGGCCCGGAAATCCAAATGGACTGCCTAGTCCTAGGCTAGATGGGAGT
AGTCCAGTGAGATCCAATAGTTCTGCCCCACCTTACATCTGTCAAATCCCCAAAATA
TTCATCGCCTATCCTAGGAGTAAAATGAATGTTATTGCATCGATGACCGTTGGTTTAC
CATGTGAACGAGAGCAATGTCACCTGTCAATCATTTCCTTGTCTTACTCTCGATGAT
CACAAAGTCAGTGGGGCTCCTTAGATTCCCTGATCCTGATATTCAGGCGAAAGGAC
TGGTCAGGGAGTGAATATGGAACTTGGGGTATTGACATAATTTATGTTGATCCTAAA
TACTCTGGAGGTAGAAATCCCAAGCATGAGCTTGTTCCCCTAGTTTCGGAACCTGA
AATGGATCTCTGATATAACTTCGGAATGTGATGCCCCTTTCCCCAACCTGTGTTTTTG

AATTTTGACTGGAATATATTCTTGGTGTTTGCTTACATCTCTCCGTTTGAACTTGGTC
TTTTGCTCTTTGTTCTTTCACGCTTCGATTATCCCTCTTCAAAGACACC

(c)

ACTGGTCTACTCGAGCCCCTAAACGTCCGACTTCGTAGCTCCCTTCGAATGTGTAA
ATTCATCTGCATCACATATCAAAACCACACTACATTCCTCACTACTATCCGATCTTCA
GCTACCTTTTACTGATACGTTGAATTCCAATAAACCTTAATCCAAAATGGTATCTTCC
AAAGAGTTTTATTCTGATCTCTAGTGGTTGAGAGGTGCGTTACAATAGCATGCGAA
AATCCAAGTTTCCTCCTTGAAGTTTCATTATGAATAAAGGGTCTATTTAAGAGAAAT
AAATAACATAAAGGCGTGGTAGAGGGGTTTTCAG

Figure 2.6. Sequences used for vector construction. (a) The 867 bp *sdhB* gene coding sequence. A mutant version containing a point mutation of the highlighted residue to thymine confers carboxin resistance and was used as a selection marker. (b) The 786 bp *sdhB* promoter sequence cloned from the 5' upstream region of *sdhB*. (c) The 319 bp *sdhB* terminator sequence cloned from the 3' downstream region of *sdhB*.

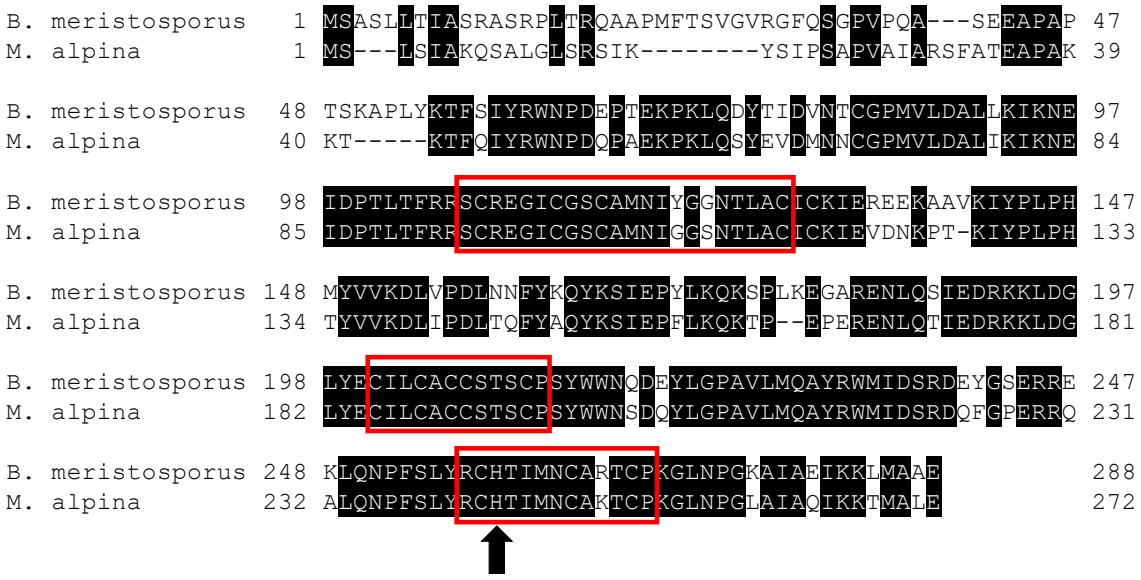

Figure 2.7. Comparison of *B. meristosporus* and *M. alpina* SDHB amino acid sequences. Red boxes show the three cysteine rich clusters. Arrow indicates the histidine residue that is substituted for leucine to confer carboxin resistance in *B. meristosporus*.

Using the templates and primers shown in **Table 2.3** (sdhBp_fwd to sdhBt2_rev), a plasmid vector based on the pBIG35ZhGUSm backbone (35), pBIG_CarR_GUSm (**Figure 2.8**), was constructed. pBIG_CarR_GUSm contained two separate cassettes regulating the expression of *CarR* and *GUSm* via their respective *sdhB* promoter and *sdhB* terminator sequences. The plasmid also contained the ColE1 and oriV origin of replication, which are capable of inducing plasmid replication in bacteria.

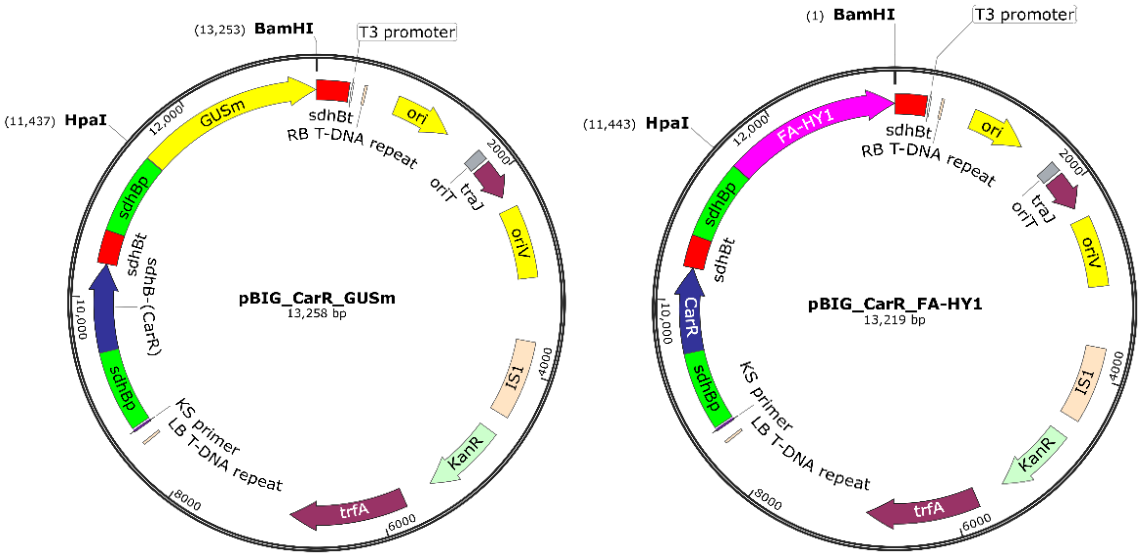

Figure 2.8. The expression vectors constructed in this study. *GUSm*, codon-optimized β-glucuronidase gene; *sdhB*p, *B. meristosporus sdhB* promoter; *sdhB*t, *B. meristosporus sdhB* terminator; *CarR*, *B. meristosporus* mutant *sdhB* gene; trfA, trfA locus which produces two proteins that promote replication of the plasmid; ori, ColEI origin of replication; oriV, pRK2 origin of replication; RB, right border; LB, left border.

Biolistic transformation

pBIG_CarR_GUSm was then introduced to *B. meristosporus* ballistospores by biolistic bombardment. After passaging the colonies for 4 generations on fresh selective media to ensure genetic stability, 142 carboxin-resistant colonies were obtained, and randomly selected colonies showed varying speed of growth on carboxin-supplemented PDA (**Figure 2.9a**). Assuming all carboxin-resistant colonies are transformants, this corresponded to a transformation efficiency of approximately 14 transformants/µg plasmid DNA and approximately 237 transformants/10^6 ballistospores.

GUS catalyzes the hydrolysis of 4-methylumbelliferyl-β-D-glucuronide (MUG) to the fluorescent 4-methylumbelliferone; MUG is therefore used in colorimetric assays to confirm stable GUS expression (36). After incubation on PDA plates supplemented with 100 µg mL^{-1} MUG for two days, the majority of carboxin resistant colonies emitted visible blue-violet light when exposed to UV light, as opposed to the WT strain which showed negligible fluorescence (**Figure 2.9b**).

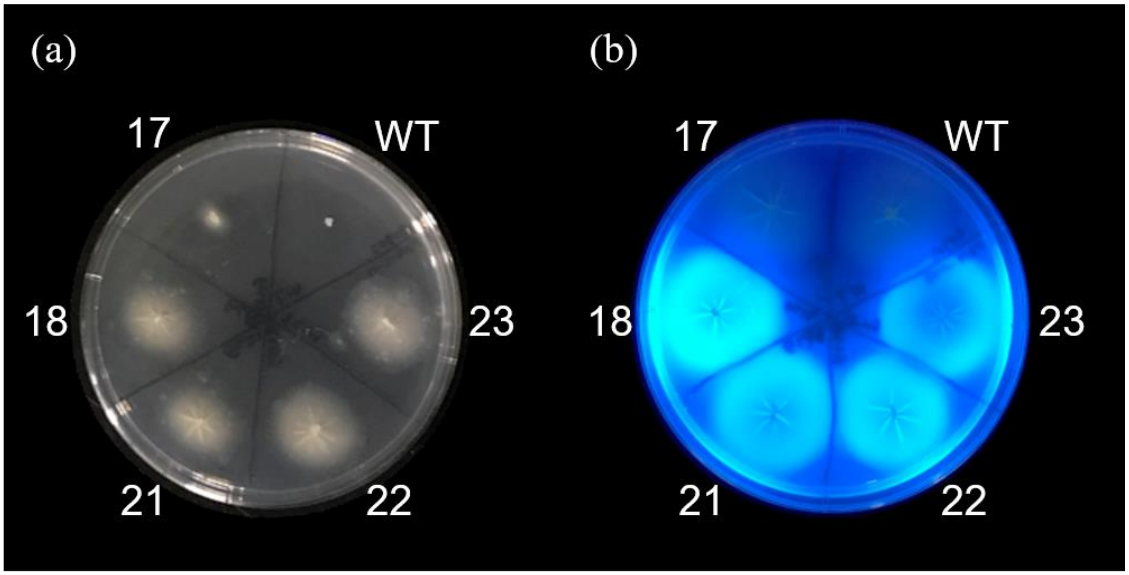

Figure 2.9. *GUSm* transformants showing (a) resistance to 100 µg mL^{-1} carboxin and (b) blue-violet fluorescence under UV light after incubation on PDA supplemented with 100µg mL^{-1} MUG.

Quantitation of GUS activity in the crude protein extracts of *GUSm* transformants by a colorimetric GUS assay showed that the majority of transformants produced significantly more *p*-nitrophenol (PNP) than the WT (**Figure 2.10a**). These results showed that *GUSm* was successfully expressed in the target cells.

To confirm that the *GUSm* was indeed present in the genomic DNA of the transformants, a *GUSm* specific primer pair (**Table 2.2**, GUSm_probe_fwd2 and GUSm_probe_rev2) was used to amplify a 1600 bp stretch of *GUSm* from pBIG_CarR_GUSm, pBIG_CarR_FA-HY1 (A pBIG_CarR_GUSm vector containing a different gene in place of *GUSm*), WT gDNA, *GUSm* transformant 3 gDNA and *GUSm*

transformant 10 gDNA. The results (**Figure 2.10b**) showed that no amplified DNA was observed for pBIG_CarR_FA-HY1 or WT gDNA, while a single band corresponding to approximately 1600 bp was amplified from pBIG_CarR_GUSm, *GUSm* transformant 3 gDNA, and *GUSm* transformant 10 gDNA. Collectively, these results demonstrate that *GUSm* was successfully transformed and expressed in *B. meristosporus* NBRC 108890.

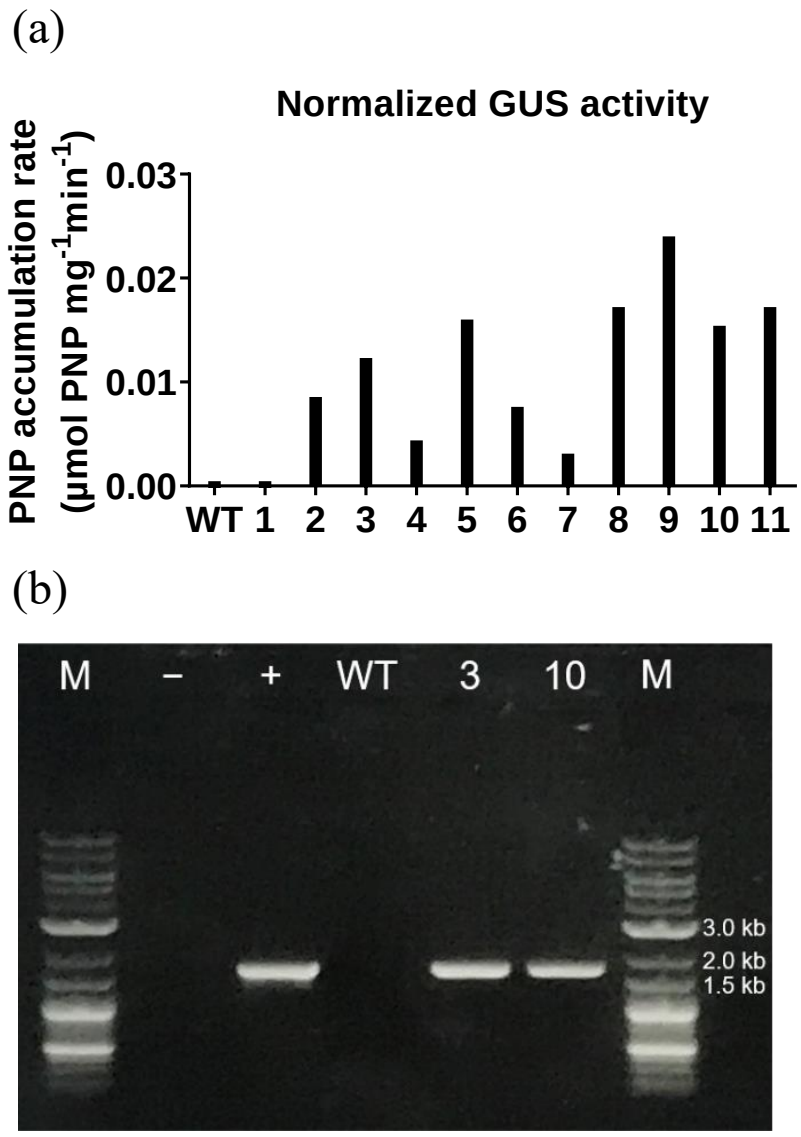

Figure 2.10. *GUSm* transformants showing (a) high PNP accumulation and (b) amplification of the *GUSm* gene from genomic DNA. M, 2-log ladder; −, pBIG_CarR_GUSm; +, pBIG_CarR_FA-HY1; WT, WT; 3, *GUSm* transformant 3; 10, *GUSm* transformant 10.

FA-HY1 ***catalyzed heterologous production of 13-hydroxy-cis-9-octadecenoic acid***

Staining of 162 h-old mycelium by the Nile red method showed that the majority of fatty acids which mainly consist of FFAs (Refer to chapter 2.1) existed as lipid droplet-like organelles inside the mycelium (**Figure 2.11**).

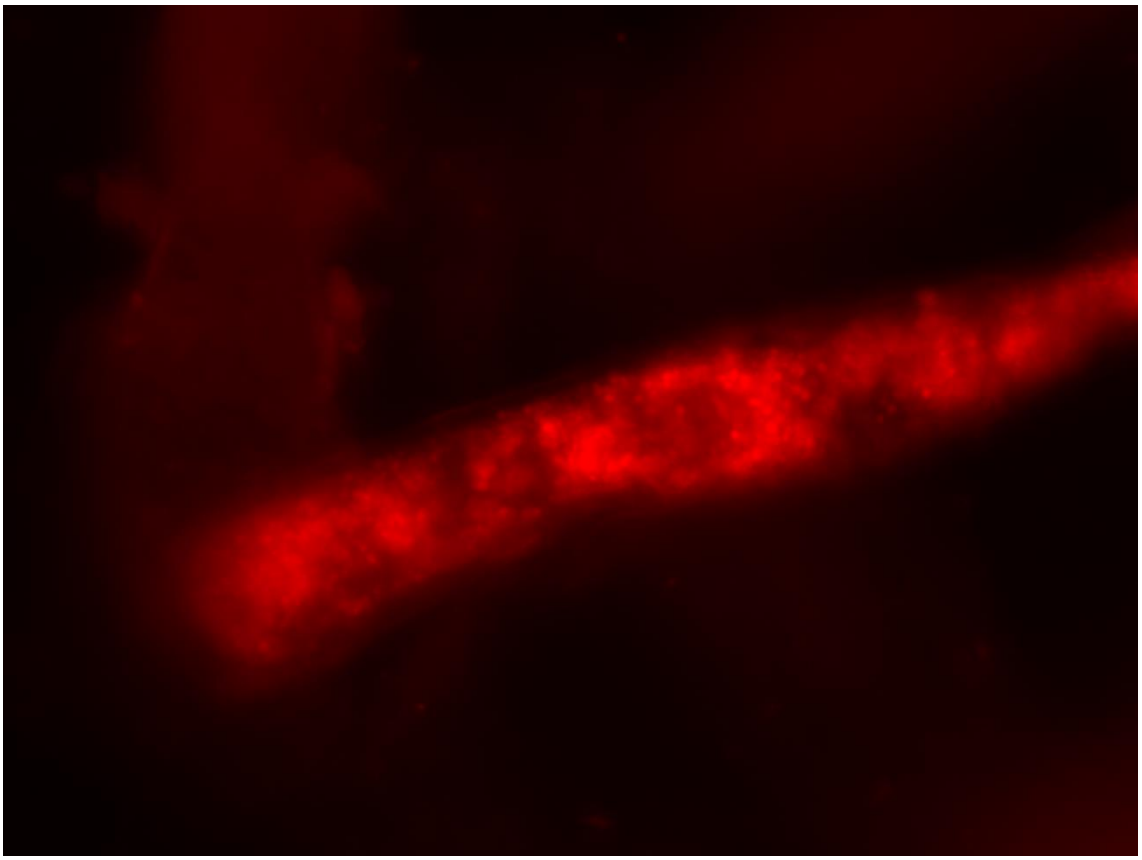

Figure 2.11. Fluorescence microscopy of *B. meristosporus* mycelium stained after Nile red lipid staining.

To demonstrate that endogenously accumulated FFAs could be utilized as substrates for FFA derivative production, *de novo* production of the hydroxy fatty acid 13-hydroxy-*cis*-9-octadecenoic acid (13-OH LA) from glucose was attempted. *Lactobacillus acidophilus FA-HY1* catalyzes the hydration of linoleic acid (LA) to 13-OH LA (37), with biochemical characterization and homology models strongly suggesting FFAs to be the sole substrates (37, 38). Since *B. meristosporus* accumulates LA as a major FFA species (Refer to chapter 2.1), the author attempted to convert this endogenous LA FFA pool to 13-OH LA by

heterologous expression of *FA-HY1*.

The expression vector pBIG_CarR_FA-HY1 was constructed, which contained two expression cassettes driving the expression of *CarR* and *FA-HY1* (**Figure 2.8**). This vector was transformed into *B. meristosporus* ballistospores according to the previous protocol. GC-MS analysis of the intracellular lipids of a resulting transformant yielded a novel peak with a similar retention time to the 13-OH LA standard, while this peak was absent for the WT (**Figure 2.12a**). The mass spectrum of the peak produced by the *FA-HY1* transformant showed the molecular ions characteristic of 13-OH LA (**Figure 2.12b**). These results confirmed that 13-OH LA was produced by the *FA-HY1* transformant but not the WT strain.

13-OH LA production was then evaluated by fed-batch cultivation at 300 mL flask scale. During fermentation, the WT showed no 13-OH LA production and the LA FFA titer reached 1250 mg L^{-1} after 162 h (**Figure 2.13a**). In comparison, the *FA-HY1* transformant showed 13-OH LA production throughout fermentation, reaching a maximum of 311 mg L^{-1} 13-OH LA after 186 h (**Figure 2.13b**). In comparison to the WT, the *FA-HY1* transformant produced significantly less LA, reaching a maximum of 668 mg L^{-1} after 186 h. These results show that *FA-HY1* was able to catalyze the hydration of endogenous LA FFA to 13-OH LA.

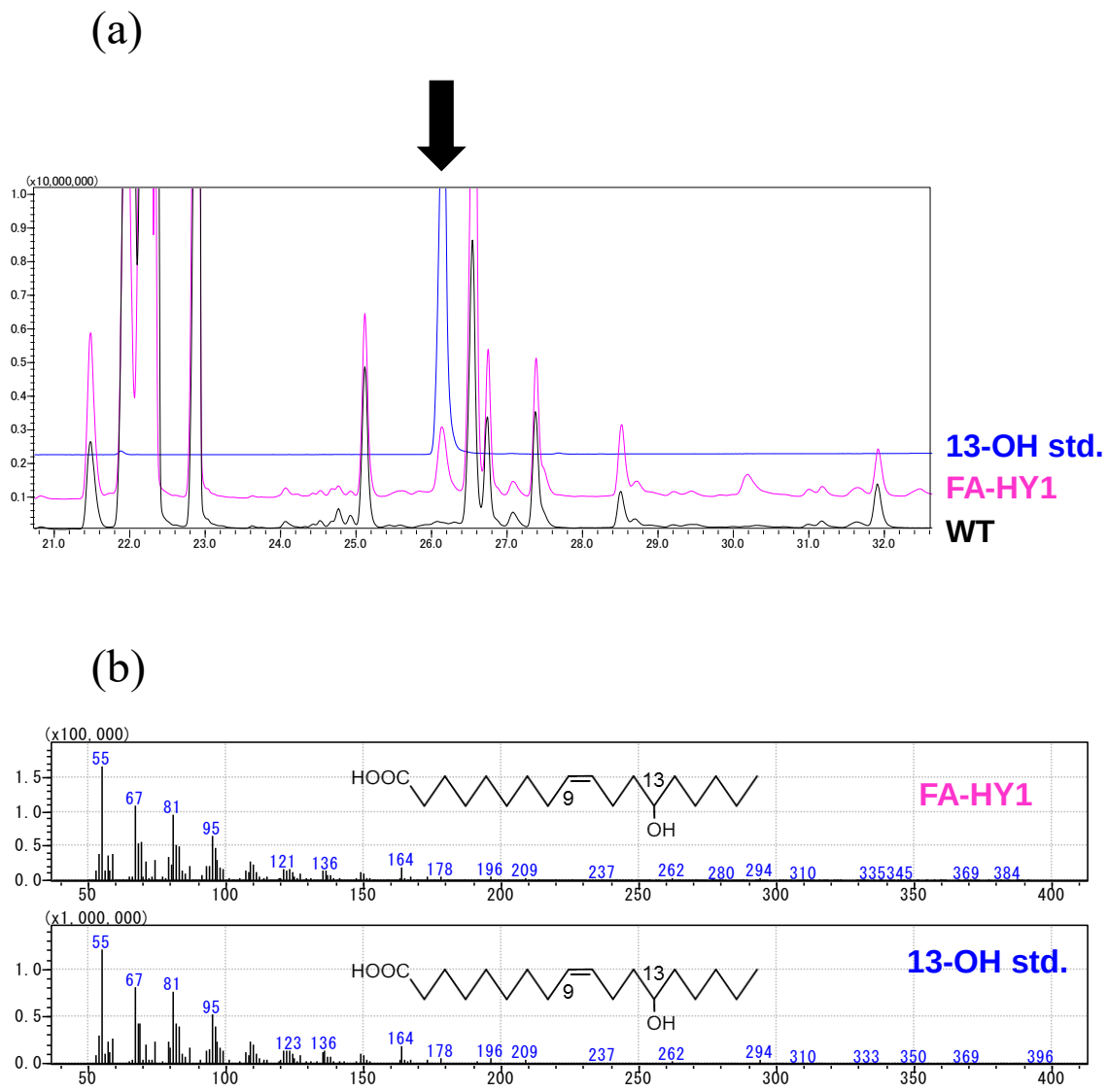

Figure 2.12. Production of 13-hydroxy-*cis*-9-octadecenoic acid (13-OH LA) by a *B. meristosporus FA-HY1* transformant (a) Gas chromatogram of WT strain, *FA-HY1* transformant and 13-OH LA standard, with the arrow showing the retention time of the 13-OH LA standard. (b) Mass spectrum of the putative 13-OH LA peak produced by the *FA-HY1* transformant compared to the 13-OH LA standard.

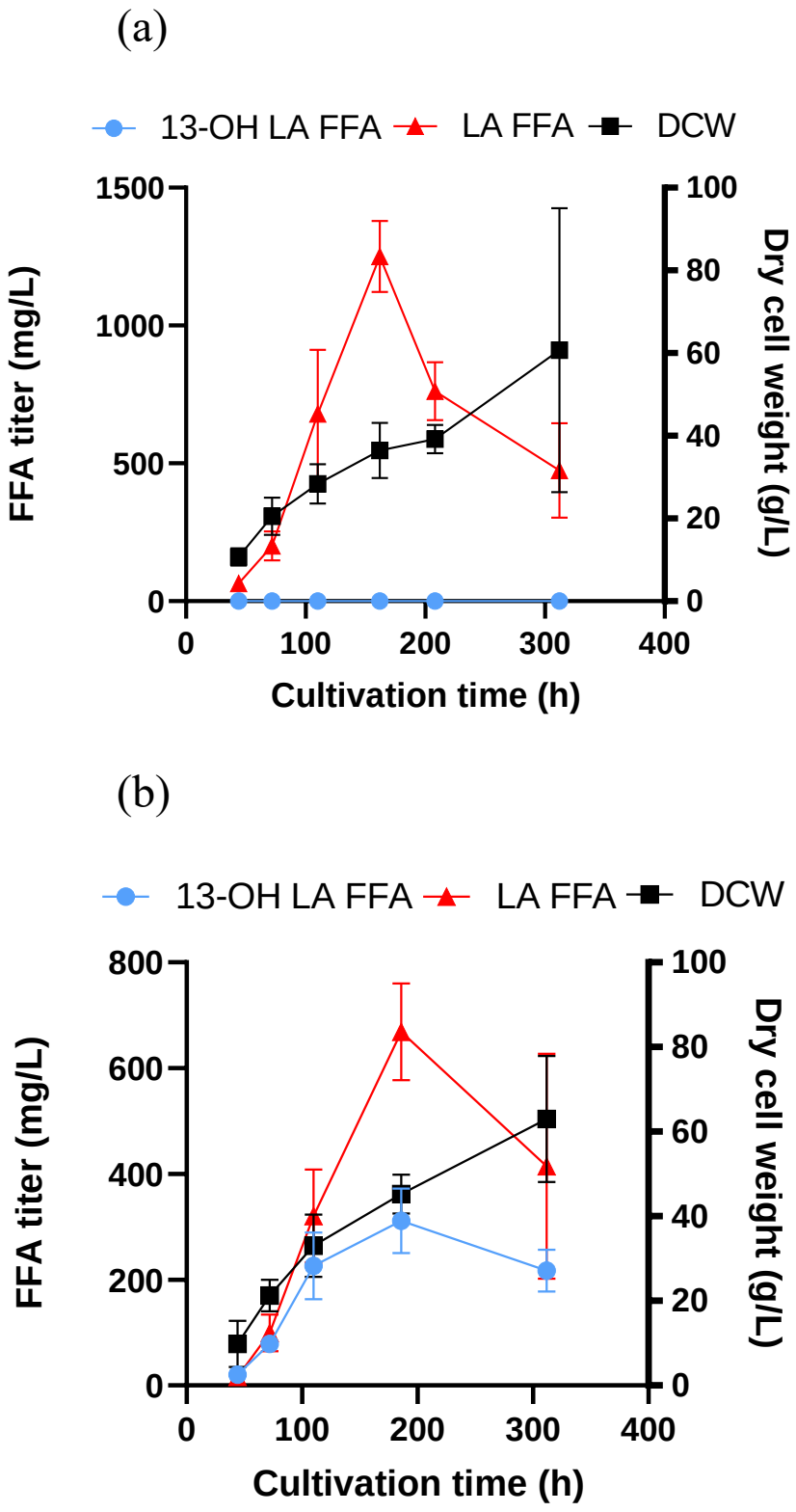

Figure 2.13. Fed-batch fermentation of 13-hydroxy-*cis*-9-octadecenoic acid by the *B. meristosporus* (a) WT strain and (b) *FA-HY1* transformant.

DISCUSSION

While the FFA producer *B. meristosporus* was previously suggested to be a potential platform for FFA-derivative production, the lack of genetic tools severely limited its application. In this study, basic genetic tools were developed that enable rapid transformation, regulation of foreign gene expression, and recovery of transformants by *CarR*-mediated carboxin resistance.

Although numerous fungal transformation protocols utilize protoplast mediated transformation (39), an efficient transformation system utilizing untreated cells was desirable to eliminate the time-consuming process of protoplast preparation. Ballistospores were particularly desirable as $>10^6$ spores could be generated and harvested easily with only a single cultivation, centrifugation, and resuspension step, which would also allow quantification of transformation efficiency and trivial colony isolation. As various filamentous fungi can be transformed by *Agrobacterium tumefaciens*-mediated transformation (ATMT) (40), preliminary experiments were conducted using the *A. tumefaciens* strains EHA105 and GV2101::PMP90, but no transformants were produced from a total of 10^6 spores (data not shown). This may have been due to low transformation efficiency or innate recalcitrance to T-DNA transfer, as ATMT transformation efficiencies for different filamentous fungi were reported to range from 1-5000/10^7 spores (40). Regardless of whether or not *B. meristosporus* can be transformed by ATMT, routine preparation of $>10^7$ spores was too laborious for future high throughput experiments, therefore higher spore concentrations were not examined.

Biolistic bombardment was thus examined as efficient transformation has been reported for a variety of cell types (39). As a result, transformants were obtained which most likely arose from chromosomal integration of plasmid DNA, since pBIG_CarR_GUSm lacks a fungal origin of replication. 142 stable transformants were isolated from a total of 6 plates containing a total of 1.2×10^6 spores, representing a transformation efficiency of 237 transformants/10^6 spores. The transformation efficiency of 237 transformants/10^6 spores represented a several-thousand fold increase in transformation efficiency compared to the biolistic transformation efficiency of *M. alpina* (50 transformants/10^8 spores) (30). Using this protocol, several thousand transformants may be feasibly obtained within a week, presenting opportunities for high-throughput applications such as functional genomic study. Transformation efficiency could potentially be further increased by optimizing other

biological and instrumental factors. To the best of the authors knowledge, this represents the first report of genetic transformation in the fungal phylum Entomophthoromycota, which contains over 250 species of pathogenic and saprobic fungi with widespread applications as cell factories and in the biological control of crop and forest pests (41, 42).

The promoter and terminator sequences used as gene expression elements were cloned from the endogenous upstream and downstream sequences of the cloned succinate dehydrogenase iron-sulfur subunit gene *sdhB,* which is an integral part of the citric acid cycle and the electron transport chain. The extent to which they initiate and terminate transcription is unclear as limited reports to date utilized *sdhB* related sequences for transgene expression and their effects on gene expression were not characterized in this study. Nevertheless, these expression elements were able to facilitate detectable expression of the transgenes *CarR, GUSm* and *FA-HY1*, which was sufficient for the purposes of this study. Future studies that necessitate optimal gene expression will require rational design of gene expression cassettes that take into account various factors such as transcription initiation, elongation rate affected by codon bias (43), and termination efficiency on protein synthesis rate.

In a previous study, the localization of endogenous FFAs in *B. meristosporus* was unclear, causing doubts about their efficient utilization as substrates by cytosolic enzymes (Refer to chapter 2.1). In this study, Nile red lipid staining apparently showed that the majority of intracellular lipids (which contains mostly FFAs) were located throughout the cytosol as lipid droplet-like organelles (**Figure 2.11**), which is surprising as only TAGs to date have been reported as a major component of lipid droplets (44). Although *FA-HY1* expression showed that FFAs could be utilized by cytosolic enzymes, the effect of FFA localization on enzyme accessibility is unclear and should be elucidated. Regardless, the *FA-HY1* transformant produced in this study represents the first report of *de novo* biosynthesis of 13-OH LA and is one of a few reports to date of hydroxy fatty acid production from glucose.

MATERIALS AND METHODS

B. meristosporus sporogenesis, harvest, and preservation

Basidiobolus meristosporus NBRC 108890 was purchased from the NITE Biotechnology Resource Center (Tokyo, Japan). Ballistospores were produced by transferring 20 3mm mycelial agar discs containing fresh growth of *B. meristosporus* on potato dextrose agar (PDA, 39 g L^{-1} potato dextrose agar) to each of five 150 mm PDA plates and incubating them inverted at 28 °C for five days. 15 mL 0.05% Tween 80 was deposited on each plate lid and the spores were dislodged very gently with a plastic spreader. The spore solution was deposited to a 50 mL centrifuge tube and the plate lid was washed with an additional 15 mL 0.05% Tween 80. The remaining spore solution was again deposited to the tube, and the harvested solution from all 5 plates was centrifuged in a bucket centrifuge at 3000 × *g* for 10 mins. The supernatant was discarded, and the spores were suspended in sterile H_2O to a concentration of 10^6 spores mL^{-1} in preparation for transformation or preservation. For spore preservation, the spore solution was mixed with 30% sterile glycerol at a ratio of 1:1. The glycerol stock was then vortexed thoroughly and stored at -80 ºC.

Lipid staining by Nile Red

Technical grade Nile Red (Sigma-Aldrich, USA) was dissolved in acetone to a final concentration of 1 mg mL^{-1}, and further dissolved in phosphate buffered saline (Sigma-Aldrich, USA) to a concentration of 20 µg mL^{-1}. 60 µL was then added to 112 h-old mycelium (Refer to "Fed-batch culture conditions") and incubated at 28 ºC with 300 strokes min^{-1} shaking for 10 mins. Stained mycelium was visualized by a Keyence BZ-X810 All-in-One Fluorescence Microscope (Osaka, Japan) equipped with BZ-X filter TRITC.

Antibiotic and fungicide susceptibility testing

3 mm PDA agar discs containing two-day-old mycelial growth were plated on 90 mm PDA agar plates containing antibiotics or fungicides at various concentrations (50, 100, 150, 200 µg mL^{-1}) and statically incubated at 28 ºC for 5 days.

Genomic DNA and RNA extraction, cDNA library preparation

For preparation of cells, a 3 mm PDA disc containing two-day-old mycelial growth was incubated to 100 mL of GY medium (2% glucose, 1% Bacto yeast extract) in a 300 mL Erlenmeyer flask (IWAKI, Japan) and incubated for 7 days at 28 ºC with shaking at 140 strokes min^{-1}. The mycelial growth was concentrated by vacuum filtration and freeze dried for 36 h using a freeze drier (EYELA, Japan).

For DNA extraction, 40 mg of dried cells were homogenized in a 1.5 mL bead-shocking tube with glass beads using a multi bead shocker (Yasui Kikai, Osaka, Japan) at 5000 strokes min^{-1} for 3 mins with 30 s break between each minute. 1.5 mL of Suisui-S extraction buffer was then added (Rizo, Japan), the mixture was inverted until homogenous, incubated for 10 mins at room temperature, and centrifuged for 10 mins at 35000 × *g*. 1.3 mL supernatant was transferred to a 2 mL Eppendorf tube, and 0.7mL phenol/chloroform/isoamyl alcohol (25:24:1) was then added. The mixture was mixed by inversion for 30 seconds and centrifuged for 5 mins at 35000 × *g*. 1.1 mL of the top aqueous layer was transferred to a new 2 mL Eppendorf tube. 0.1 volume of 3 M NaAc (pH 5.5) and 0.7 volume of isopropanol was added, and the mixture was incubated at -20 ºC for 20 mins, then centrifuged at 35000 × *g* for 10 mins. The supernatant was discarded by decantation and the pellet was washed twice with 1 mL 70% ethanol. The 70% ethanol was pipetted off, and the residual moisture was blotted from the pellet using a Kimwipe and the pellet was incubated at RT for 2 mins. The nucleic acid pellet was then dissolved in 50 µL of water and 40 µg RNase A (Nippon gene, Japan) and incubated at 37 ºC for one hour. Then DNA was then repurified by phenol/chloroform/isoamyl alcohol and precipitated by isopropanol as previously described.

RNA was extracted from 100 mg of dried cells using the Nucleospin plant kit (Macherey-Nagel, Germany) according the user manual. The corresponding cDNA library was constructed using the SMARTer RACE 5'/3' kit (Takara Bio USA Inc, USA).

Cloning of *CarR, sdhB* promoter, and *sdhB* terminator

For sequencing of the *B. meristosporus sdhB* gene, a reverse gene specific primer was designed (**Table 2.2**, sdhB_3UTR_2_RV_P2) to anneal to the 3' UTR of the *B. meristosporus* NBRC 108890 *sdhB* sequence based on the NCBI gene sequence of the hypothetical succinate dehydrogenase iron-sulfur protein of *B. meristosporus* CBS 931.73 (accession number: ORX89895.1). Touchdown PCR was performed according to the user

manual using this reverse gene specific primer and the Takara SMARTer universal primer UPM which anneals at the 5' end of the cDNA. A resulting band approximately 1.2 kb long was purified by agarose gel excision, cloned into a pUC118 plasmid vector using the Blunt End Mighty Cloning Reagent Set (Takara, Japan), and sequenced, yielding the 867 bp *sdhB* coding sequence (**Figure 2.6a**). The adenine residue at position 776 was then mutated to thymine by overlap extension PCR and the resulting plasmid containing the 867 bp *CarR* sequence was designated pUC118_CarR.

For cloning and sequencing of the *sdhB* promoter, a forward primer approximately 800 bp upstream of the hypothetical *sdhB* sequence of *B. meristosporus* CBS 931.73 (Accession number: ORX89895.1) and a reverse primer based on the *B. meristosporus* NBRC 108890 *sdhB* gene (**Table 2.2**, sdhBp-800fwd and sdhBp+50rev) was used to amplify a putative *sdhB* promoter sequence from 20 ng *B. meristosporus* NBRC 108890 genomic DNA. PCR was performed by one cycle of 94 ºC for 2 mins then 30 cycles each consisting of 98 ºC for 10 s, 61 ºC for 30 s, and 68 ºC for 45 s using KOD FX Neo (Toyobo, Japan). A resulting band approximately 0.9 kb long was cloned into a pUC118 plasmid vector using the Blunt End Mighty Cloning Reagent Set (Takara, Japan) and designated pUC118_sdhBp. Sanger sequencing of the insert yielded a putative 786 bp promoter sequence (**Figure 2.6b**).

For cloning and sequencing of the *sdhB* terminator, a forward primer based on the sequenced NBRC 108890 *sdhB* gene and a backward primer based on the downstream sequence of the hypothetical *sdhB* gene of *B. meristosporus* CBS 931.73 (accession number: ORX89895.1) were designed (**Table 2.2**, sdhBt_BamHI_fwd and sdhBt_NheI_rev). Using 20 ng genomic DNA as template, PCR was performed by one cycle of 94 ºC for 2 mins then 30

Table 2.2 Primers used for cloning of *sdhB*, *sdhB* promoter, *sdhB* terminator and the *GUSm* probe.

Primer name	Template	Sequence
sdhB_3UTR_2_RV_P2	WT cDNA library	5' gcttggataggaaattctgctatggggatgggtg 3'
sdhBp-800fwd sdhBp+50rev	WT genomic DNA	5' attctcggttaggaagttgacttgacag 3' 5' gtctagtgagcggtctggaagctc 3'
sdhBt_BamHI_fwd sdhBt_NheI_rev	WT genomic DNA	5' ggatccactggtctactcgagcccctaaacg 3' 5' gctagcctgaaaaccctctaccacgcc 3'
GUSm_probe_fwd2 GUSm_probe_rev2	WT genomic DNA/ pBIG35ZhGUSm (35)	5' gagatcaagaagctcgacggcctctgg 3' 5' cgacggccgagacacggtcaaaga 3'

cycles each consisting of 98 ºC for 10 s, 60 ºC for 30 s, and 68 ºC for 30 s using KOD FX Neo (Toyobo, Japan). The resulting 0.4 kb band was cloned into a pUC118 plasmid vector using the Blunt End Mighty Cloning Reagent Set (Takara, Japan) and designated pUC118_sdhBt. Sanger sequencing of the insert yielded a putative 319 bp terminator sequence (**Figure 2.6c**).

Plasmid vector construction for *CarR, GUSm,* and *FA-HY1* expression

For construction of the plasmid vector driving expression of the mutant succinate dehydrogenase gene *CarR* and the expression marker gene *GUSm*, 14 primers were designed to amplify 7 fragments (**Table 2.3**, pBIG_backbone_fwd to sdhBt2_rev). These fragments were joined to form a circular vector using HiFi DNA Assembly (New England Biolabs, USA) and designated pBIG_CarR_GUSm (**Figure 2.8**).

For construction of the plasmid containing *CarR* and the *L. acidophilus* fatty acid hydratase *FA-HY1*, a codon-optimized version of *FA-HY1* was first synthesized and amplified using a primer pair designed to add on *Hpa* I at the 5' end and *Bam*HI at the 3' end (**Table 2.3**, HpaI_FA-HY1_BamHI_fwd and HpaI_FA-HY1_BamHI_rev). The amplified fragment was digested with *Hpa*I and *Bam*HI and cloned into the *Hpa*I/*Bam*HI digested pBIG_CarR_GUSm plasmid vector. The resulting vector was designated pBIG_CarR_FA-HY1 (**Figure 2.8**).

Table 2.3 Primers used for construction of the plasmid vectors pBIG_CarR_GUSm and pBIG_CarR_FA-HY1.

Primer name	Template	Fragment length (bp)	Primer sequence
pBIG_backbone_fwd pBIG_backbone_rev	pBIG35ZhGUSm (35)	8383	5' gaggggttttcaggagctccagcttttgttc 3' 5' cctaaccgagaatgaattcgatatcaagcttatcg 3'
sdhBp_fwd sdhB_rev	pUC118_sdhBp	798	5' gatatcgaattcattctcggttaggaagttg 3' 5' ggtgtctttgaagagggataatc 3'
CarR_fwd CarR_rev	pUC118_CarR	905	5' tcgattatccctcttcaaagacaccatgtcagcctcacttttg 3' 5' cgagtagaccagtttattcggctgccatcaac 3'
sdhBt_fwd sdhBt_rev	pUC118_sdhBt	343	5' gcagccgaataaactggtctactcgagccc 3' 5' ctaaccgagaatctgaaaacccctctaccac 3'
sdhBp2_fwd sdhBp2_rev	pUC118_sdhBp	811	5' gaggggttttcagattctcggttaggaagttg 3' 5' gagcatgttaacggtgtctttgaagagggataatc 3'
GUSm_fwd GUSm_rev	pBIG35ZhGUSm (35)	1850	5' cttcaaagacaccgttaacatgctccgccccgtcgag 3' 5' cgagtagaccagtggatccttactgcttgccgccctgc 3'
sdhBt2_fwd sdhBt2_rev	pUC118_sdhBt	343	5' cagtaaggatccactggtctactcgagccc 3' 5' aagctggagctcctgaaaacccctctaccac 3'
HpaI_FA-HY1_BamHI_fwd HpaI_FA-HY1_BamHI_rev	Codon-optimized *FA-HY1*	1786	5' gggaattcgttaacatgcactactcctccggtaactacga 3' 5' gaattcccggatccttagaccaacttgtacttcttcaacaactcc 3'

Biolistic transformation

2×10^5 ballistospores were plated directly to the center of each of six 90 mm PDA plates supplemented with 100μg mL^{-1} carboxin (TCI, Japan). For 12 bombardments, 6 mg tungsten carriers (1.1 μm diameter, Bio-Rad, USA) were coated with 10 μg pBIG_CarR_GUSm according to the Biolistic PDS-1000/He Particle Delivery System user manual (Bio-rad). Each plate was bombarded twice with a target distance of 6 cm, 28 in. Hg vacuum and 1,100 psi helium rupture pressure. 100 μL sterile H_2O was then added and the spores were dispersed evenly over the surface of the agar using a plastic spreader. The plates were incubated inverted at 28 ºC for three days, and resulting colonies were passaged for four cycles to fresh PDA plates supplemented with 100 μg mL^{-1} carboxin.

Confirmation and quantification of GUS activity by GUS assay

Colonies that showed carboxin resistance were checked for GUS activity by visual confirmation of fluorescence under UV light after incubation on PDA medium supplemented with 100 μg mL^{-1} MUG.

Preparation of crude protein extracts and GUS assays were performed as previously described (35, 36).

To confirm the presence of *GUSm* in the DNA of pBIG_CarR_GUSm transformants, a primer pair (**Table 2.2**, GUSm_probe_fwd2 and GUSm_probe_rev2) was used to amplify a GUSm specific stretch of DNA from WT genomic DNA, GUSm transformant genomic DNA, with pBIG_CarR_GUSm as a positive control and pBIG_CarR_FA-HY1 as a negative control.

Fed-batch culture conditions

Fed-batch fermentations of the WT strain and FA-HY1 transformant were carried out using 15 mL of GP44 medium (4% glucose and 4% Hipolypepton S [Nihon Pharmaceutical, Japan], initial pH adjusted to 7 and autoclaved) in 300 mL baffled Erlenmeyer flasks (Sibata, Japan) with silicone caps (Model C-40, AS ONE, Japan) at 28 °C, with shaking at 90 strokes min^{-1} in a rotary shaker. 937.5 μL 64% glucose and 1875 μL 32% Hipolypepton S were supplemented at 62, 88, 112, 138, and 162 h. 1875 μL 64% glucose and 3750 μL 32% Hipolypepton S were supplemented at 187 and 258 h.

Time point glucose measurement

Medium residual glucose levels were quantified with the WAKO glucose II kit (Wako, Japan).

Dry cell weight measurements, lipid extraction, and FFA analysis by gas chromatography

Mycelial time point samples for lipid quantification were stored at -20 °C for lipid titer analysis. Mycelium was harvested by vacuum filtration and freeze dried for 36 h using a freeze dryer (EYELA, Japan). Dry cell weight was then measured by a mechanical scale.

For lipid extraction, approximately 50 mg of dried cells were used and the ratio of used cells/total cells was recorded for calculation of total fatty acid titer. The cells were transferred to a bead-beating tube (WATSON, Japan) and beaten with 1 mL of added water at 4000 × *g* for 2 mins. The lipids were extracted by the Bligh and Dyer method as previously stated (7) with 0.5 mg of tricosanoic acid as an internal standard. Approximately 1 mg lipids were transferred to test tubes and analyzed by a modified version of a method utilizing trimethylsilyldiazomethane described previously (7). The lipids were dissolved in 5 mL methanol/benzene (2:3) and methylated with 150 µL 1% trimethylsilyldiazomethane in hexane at 28 °C for 30 mins. The resulting fatty acid methyl esters were analyzed by GLC as previously stated (7). FFA concentration was calculated by the corresponding fatty acid/internal standard peak area. For the calculation of FFA titer, the sum of the initial medium volume and the fed solution volume was used.

REFERENCES

1. IPCC, *Climate change 2014: synthesis report* (2014).
2. United Nations Environment Programme, “Emissions Gap Report 2019” (2019).
3. J. D. Keasling, Manufacturing molecules through metabolic engineering. *Science (80-.).* **330**, 1355–1358 (2010).
4. Y. Tsuchiya, U. Pham, I. Gout, Methods for measuring CoA and CoA derivatives in biological samples. *Biochem. Soc. Trans.* **42**, 1107–1111 (2014).
5. A. Q. Yu, N. K. Pratomo Juwono, S. S. J. Leong, M. W. Chang, Production of fatty acid-derived valuable chemicals in synthetic microbes. *Front. Bioeng. Biotechnol.* **2**, 1–12 (2014).
6. H. Furumoto, *et al.*, 10-Oxo-trans-11-octadecenoic acid generated from linoleic acid by a gut lactic acid bacterium *Lactobacillus plantarum* is cytoprotective against oxidative stress. *Toxicol. Appl. Pharmacol.* **296**, 1–9 (2016).
7. S. Kishino, *et al.*, Polyunsaturated fatty acid saturation by gut lactic acid bacteria affecting host lipid composition. *Proc. Natl. Acad. Sci. U. S. A.* **110**, 17808–17813 (2013).
8. J. Miyamoto, *et al.*, A gut microbial metabolite of linoleic acid, 10-hydroxy-cis-12-octadecenoic acid, ameliorates intestinal epithelial barrier impairment partially via GPR40-MEK-ERK pathway. *J. Biol. Chem.* **290**, 2902–2918 (2015).
9. K. R. Kim, D. K. Oh, Production of hydroxy fatty acids by microbial fatty acid-hydroxylation enzymes. *Biotechnol. Adv.* **31**, 1473–1485 (2013).
10. Y. C. Joo, *et al.*, Production of 10-hydroxystearic acid from oleic acid by whole cells of recombinant Escherichia coli containing oleate hydratase from *Stenotrophomonas maltophilia*. *J. Biotechnol.* **158**, 17–23 (2012).
11. M. Takeuchi, *et al.*, Efficient enzymatic production of hydroxy fatty acids by linoleic acid Δ9 hydratase from *Lactobacillus plantarum* AKU 1009a. *J. Appl. Microbiol.* **120**, 1282–1288 (2016).
12. E. Y. Jeon, *et al.*, Bioprocess engineering to produce 10-hydroxystearic acid from oleic acid by recombinant *Escherichia coli* expressing the oleate hydratase gene of *Stenotrophomonas maltophilia*. *Process Biochem.* **47**, 941–947 (2012).

13. C. Sung, *et al.*, The production of ω-hydroxy palmitic acid using fatty acid metabolism and cofactor optimization in *Escherichia coli*. *Appl. Microbiol. Biotechnol.* **99**, 6667–6676 (2015).
14. X. Wang, *et al.*, Biosynthesis of long chain hydroxyfatty acids from glucose by engineered *Escherichia coli*. *Bioresour. Technol.* **114**, 561–566 (2012).
15. K. Xiao, *et al.*, Metabolic engineering for enhanced medium chain omega hydroxy fatty acid production in *Escherichia coli*. *Front. Microbiol.* **9** (2018).
16. C. H. Bowen, J. Bonin, A. Kogler, C. Barba-Ostria, F. Zhang, Engineering *Escherichia coli* for conversion of glucose to medium-chain *ω*-hydroxy fatty acids and *α,ω*-dicarboxylic acids. *ACS Synth. Biol.* **5**, 200–206 (2016).
17. Y. Cao, *et al.*, Metabolic engineering of *Escherichia coli* for the production of hydroxy fatty acids from glucose. *BMC Biotechnol.* **16**, 1–9 (2016).
18. J. Liu, C. Zhang, W. Lu, Biosynthesis of long-chain ω-hydroxy fatty acids by engineered *Saccharomyces cerevisiae*. *J. Agric. Food Chem.* **67**, 4545–4552 (2019).
19. H. J. Janßen, A. Steinbüchel, Fatty acid synthesis in *Escherichia coli* and its applications towards the production of fatty acid based biofuels. *Biotechnol. Biofuels* **7**, 1–26 (2014).
20. O. Tehlivets, K. Scheuringer, S. D. Kohlwein, Fatty acid synthesis and elongation in yeast. *Biochim. Biophys. Acta - Mol. Cell Biol. Lipids* **1771**, 255–270 (2007).
21. J. Sheng, X. Feng, Metabolic engineering of yeast to produce fatty acid-derived biofuels: Bottlenecks and solutions. *Front. Microbiol.* **6** (2015).
22. M. Dourou, D. Aggeli, S. Papanikolaou, G. Aggelis, Critical steps in carbon metabolism affecting lipid accumulation and their regulation in oleaginous microorganisms. *Appl. Microbiol. Biotechnol.* **102**, 2509–2523 (2018).
23. D. Xie, Integrating cellular and bioprocess engineering in the non-conventional yeast *Yarrowia lipolytica* for biodiesel production: A review. *Front. Bioeng. Biotechnol.* **5** (2017).
24. H. M. Alvarez, *et al.*, Insights into the metabolism of oleaginous *Rhodococcus* spp. *Appl. Environ. Microbiol.* **85**, e00498-19 (2019).
25. X. Lu, H. Vora, C. Khosla, Overproduction of free fatty acids in *E. coli*: Implications for biodiesel production. *Metab. Eng.* **10**, 333–339 (2008).
26. L. Chen, J. Zhang, J. Lee, W. N. Chen, Enhancement of free fatty acid production in

Saccharomyces cerevisiae by control of fatty acyl-CoA metabolism. *Appl. Microbiol. Biotechnol.* **98**, 6739–6750 (2014).

27. E. Y. Yuzbasheva, *et al.*, A metabolic engineering strategy for producing free fatty acids by the *Yarrowia lipolytica* yeast based on impairment of glycerol metabolism. *Biotechnol. Bioeng.* **115**, 433–443 (2018).
28. A. P. Desbois, V. J. Smith, Antibacterial free fatty acids: activities, mechanisms of action and biotechnological potential. *Appl. Microbiol. Biotechnol.* **85**, 1629–1642 (2010).
29. L. Yafetto, *et al.*, The fastest flights in nature: High-speed spore discharge mechanisms among fungi. *PLoS One* **3**, 1–5 (2008).
30. A. Ando, E. Sakuradani, K. Horinaka, J. Ogawa, S. Shimizu, Transformation of an oleaginous zygomycete *Mortierella alpina* 1S-4 with the carboxin resistance gene conferred by mutation of the iron-sulfur subunit of succinate dehydrogenase. *Curr. Genet.* **55**, 349–356 (2009).
31. P. J. Punt, C. A. M. J. J. van den Hondel, Transformation of filamentous fungi based on hygromycin B and phleomycin resistance markers. *Methods Enzymol.* **216**, 447–457 (1992).
32. J. T. Ulrich, D. E. Mathre, Mode of action of oxathiin systemic fungicides. V. Effect on electron transport system of *Ustilago maydis* and *Saccharomyces cerevisiae*. *J. Bacteriol.* **110**, 628–632 (1972).
33. W. Skinner, *et al.*, A single amino-acid substitution in the iron-sulphur protein subunit of succinate dehydrogenase determines resistance to carboxin in *Mycosphaerella graminicola*. *Curr. Genet.* **34**, 393–398 (1998).
34. P. L. E. Broomfield, J. A. Hargreaves, A single amino-acid change in the iron-sulphur protein subunit of succinate dehydrogenase confers resistance to carboxin in *Ustilago maydis*. *Curr. Genet.* **22**, 117–121 (1992).
35. T. Okuda, *et al.*, Selection and characterization of promoters based on genomic approach for the molecular breeding of oleaginous fungus *Mortierella alpina* 1S-4. *Curr. Genet.* **60**, 183–191 (2014).
36. R. A. Jefferson, Assaying chimeric genes in plants: The GUS gene fusion system. *Plant Mol. Biol. Report.* **5**, 387–405 (1987).
37. A. Hirata, *et al.*, A novel unsaturated fatty acid hydratase toward C16 to C22 fatty acids

from *Lactobacillus acidophilus*. *J. Lipid Res.* **56**, 1340–1350 (2015).

38. B. E. Eser, *et al.*, Rational engineering of hydratase from *Lactobacillus acidophilus* reveals critical residues directing substrate specificity and regioselectivity. *ChemBioChem* **21**, 550–563 (2020).
39. D. Li, Y. Tang, J. Lin, W. Cai, Methods for genetic transformation of filamentous fungi. *Microb. Cell Fact.* **16**, 1–13 (2017).
40. M. J. A. de Groot, P. Bundock, P. J. . Hooykaas, A. G. M. Beijersbergen, *Agrobacterium tumefaciens*-mediated transformation of filamentous fungi. *Nat. Biotechnol.* **16**, 839–842 (1998).
41. A. P. Gryganskyi, *et al.*, Phylogenetic lineages in Entomophthoromycota. *Persoonia Mol. Phylogeny Evol. Fungi* **30**, 94–105 (2013).
42. D. Chandler, *Basic and applied research on entomopathogenic fungi* (Elsevier Inc., 2017) https:/doi.org/10.1016/B978-0-12-803527-6.00005-6.
43. T. E. F. Quax, N. J. Claassens, D. Söll, J. van der Oost, Codon bias as a means to fine-tune gene expression. *Mol. Cell* **59**, 149–161 (2015).
44. T. C. Walther, R. V. Farese, The life of lipid droplets. *Biochim. Biophys. Acta - Mol. Cell Biol. Lipids* **1791**, 459–466 (2009).

CONCLUSIONS

Taken altogether, the results obtained in chapter 1 show that the EPA/ARA ratio is a viable indicator for the isolation of highly efficient non-specific and C20-specific ω3 desaturases from Peronosporales and Saprolegniales species. Broader screenings utilizing this strategy for the selection of oomycetes or other organisms with similar lipid profiles should yield additional ω3 desaturases with biotechnological potential. The three ω3 desaturases that were discovered using this strategy, *psulω3*, *pmd17c*, and *pmd17g* function under ordinary temperatures and show biotechnological importance. *psulω3* is a non-specific ω3 desaturase that shows high potential for EPA production through C18 and C20 fatty acids. The discovery of *pmd17c* and *pmd17g* adds to the limited pool of C20-specific ω3 desaturases and is of great value for EPA biosynthesis in *M. alpina* via C20 ω6 PUFAs due to the ability of these enzymes to convert endogenous ω6 PUFAs to ω3 PUFAs with minimal byproducts and a high conversion efficiency. Future research may utilize this enzyme for the production of EPA by known C20 ω6 PUFA producers such as *Mortierella* spp., *Yarrowia lipolytica*, *Pythium* spp., *Diasporangium*, *Parietochloris incisa*, *Porphyridium cruentum*, and even oleaginous bacteria such as *Aureispira maritima*. The discovery of these ω3 desaturases should therefore facilitate the advent of more sustainable EPA sources.

In chapter 2.1, the results show that *B. meristosporus* NBRC 108890 has high potential for application toward bioproduction of FFA-derived oleochemicals due to its ability to utilize lignocellulose-derived carbon sources, grow rapidly to high cell densities under a wide range of conditions, and efficiently produce FFAs of industrially relevant chain length. As the wild type showed FFA production metrics superior to other reported wild type strains, it is expected that metabolic engineering and additional characterization at bioreactor scale will produce levels of FFAs superior to current platforms. Genetic engineering tools and metabolic models should be established to overexpress its FFA production pathway and heterologously produce FFA-derivatives such as next generation biofuels and oleochemicals. Furthermore, the genetic tools developed in chapter 2.2 enable rapid transformation, regulation of gene expression and transformant recovery of *B. meristosporus* NBRC 108890. Using these genetic tools, the accessibility of endogenous FFAs to cytosolic enzymes was demonstrated by the heterologous conversion of intracellular FFAs to the FFA-derivative

13-hydroxy-*cis*-9-octadecenoic acid. The discovery of this organism and development of basic genetic tools should form a cornerstone for the development of a new fungal FFA production platform and facilitate the cost-effective, sustainable production of FFA-derived oleochemicals and fuels.

ACKNOWLEDGEMENTS

The present thesis is based on the studies carried out from 2016 to 2021 at the Laboratory of Fermentation Physiology and Applied Microbiology, Division of Applied Life Sciences, Graduate School of Agriculture, Kyoto University.

I would first like to thank Professor Jun Ogawa for his unstinting support, warm encouragement, and invaluable advice throughout the course of this study.

I would also like to express my sincere gratitude to Assistant Professor Akinori Ando for his guidance and constant encouragement throughout the course of this study.

My gratitude also goes to Professor Makoto Ueda, Associate Professors Shigenobu Kishino and Ryotaro Hara, Assistant Professors Michiki Takeuchi and Hiroko Watanabe, Dr. Tomoyo Okuda, Dr. Yuta Sugiyama, Dr. Hiroshi Kikukawa, Dr. Yoshimi Shimada, Dr. Si-bum Park, Dr. Hideaki Nagano, Dr. Nahoko Kitamura, and Dr. Natsumi Okada, for their kind advice during progress discussions and seminar presentations, experimental instruction, and continuous encouragement.

I would also like to thank Mr. Yu-An Sui, Mr. Yudai Miyoshi, Dr. Mohd Fazli Bin Farida Asras, Mr. Daniel Makoto Takeuchi, Ms. Amber Bultena, and Mr. Chun Wai Hui, for their assistance with experiments and strong support.

I am grateful for the strong support of all members of my group, beginning with Mr. Shohei Katsuya, Mr. Mamoru Kida, Ms. Miku Itokawa, Mr. Mikio Kojima, Mr. Chang-Yu Wu, Mr. Liang-Wei Wei, and Ms. Tomoka Yokoi, as well as all past members.

This research would not have been successfully conducted without Ms. Atsuko Kitamura and all other members of the Laboratory of Fermentation Physiology and Applied Microbiology. Thank you.

I would also like to specially thank Jiseul Park for her endless patience and care, and for her reassurances from start to finish.

Finally, I offer my deepest gratitude to my dad, for his never-ending support and for always inspiring me to do my best; my mum, for her gentle encouragement and understanding, and my sister, for her kind words of support.

PUBLICATIONS

Brian K. H. Mo, Akinori Ando, Ryohei Nakatsuji, Tomoyo Okuda, Yuki Takemoto, Hiroyuki Ikemoto, Hiroshi Kikukawa, Takaiku Sakamoto, Eiji Sakuradani, Jun Ogawa, Characterization of ω3 fatty acid desaturases from oomycetes and their application toward eicosapentaenoic acid production in *Mortierella alpina*. *Bioscience, Biotechnology, and Biochemistry*. In Press.

Brian K. H. Mo, Akinori Ando, Tasuku Kitamoto, Hiroshi Yamaguchi, Jun Ogawa, Free fatty acid production by the oleaginous fungus *Basidiobolus meristosporus*. In preparation.

Brian K. H. Mo, Akinori Ando, Tasuku Kitamoto, Jun Ogawa, Development of a host-vector system for free fatty acid derivative production by the oleaginous fungus *Basidiobolus meristosporus*. In preparation.